Fractional QCQP with Applications in ML Steering Direction Estimation for Radar Detection

A. De Maio, Y. Huang, D. P. Palomar, S. Zhang, and A. Farina

Abstract

This paper deals with the problem of estimating the steering direction of a signal, embedded in Gaussian disturbance, under a general quadratic inequality constraint, representing the uncertainty region of the steering. We resort to the Maximum Likelihood (ML) criterion and focus on two scenarios. The former assumes that the complex amplitude of the useful signal component fluctuates from snapshot to snapshot. The latter supposes that the useful signal keeps a constant amplitude within all the snapshots. We prove that the ML criterion leads in both cases to a fractional Quadratically Constrained Quadratic Problem (QCQP). In order to solve it, we first relax the problem into a constrained fractional Semidefinite Programming (SDP) problem which is shown equivalent, via the Charnes-Cooper transformation, to an SDP problem. Then, exploiting a suitable rank-one decomposition, we show that the SDP relaxation is tight and give a procedure to construct (in polynomial time) an optimal solution of the original problem from an optimal solution of the fractional SDP. We also assess the quality of the derived estimator through a comparison between its performance and the constrained Cramer Rao lower Bound (CRB). Finally, we give two applications of the proposed theoretical framework in the context of radar detection.

Index terms. Fractional QCQP, Constrained Maximum Likelihood Steering Direction Estimation, Radar Applications.

A. De Maio is with Università degli Studi di Napoli “Federico II”, Dipartimento di Ingegneria Biomedica, Elettronica e delle Telecomunicazioni, Via Claudio 21, Napoli, Italy. E-mail: ademaio@unina.it.

Y. Huang and D. P. Palomar are with Department of Electronic and Computer Engineering, Hong Kong University of Science and Technology, Clear Water Bay, Kowloon, Hong Kong. E-mail: eeyw@ust.hk, palomar@ust.hk.

S. Zhang is with Department of Systems Engineering and Engineering Management, The Chinese University of Hong Kong, Shatin, Hong Kong. E-mail: zhang@se.cuhk.edu.hk.

A. Farina is with SELEX Sistemi Integrati, via Tiburtina Km.12.4, Roma, Italy. E-mail: afarina@selex-si.com.

I. INTRODUCTION

The problem of estimating the steering direction vector is of relevant interest in some applications concerning radar detection and beamforming. In fact, there are several physical phenomena why the received steering vector is quite often not aligned with the nominal expected direction: such as pointing errors caused by the radar antenna which forms a beam not pointed in the exact desired direction; imperfect array calibration and distorted antenna shape because of array imperfections; spatial multipath causing severe distortions in the presumed steering vector due to the presence of signals from several paths (coherent and incoherent local scattering); source wavefront distortion implied by the signal propagation through non-homogeneous media; in-phase and quadrature components errors due to unbalanced lowpass filters; A/D sampling errors; dc bias; non-linearities; and intermodulation products. In other words, there is some imperfect knowledge on the actual steering direction which is usually characterized in terms of an uncertainty region. Many adaptive radar signal processing methods that assume the exact knowledge of the signal array response vector often suffer a performance degradation, when the actual steering vector is not perfectly aligned with the nominal one (even small variations in the array manifold can reduce their performance).

In order to account for the quoted uncertainty, several estimation techniques have been proposed in open literature. For instance, with reference to beamforming applications, steering estimation is explicitly or implicitly addressed in [1], [2], [3], [4], [5]. As to the case of radar detection, steering vector estimation can be found in [6], [7], [8], [9], [10], [11], [12].

All the mentioned approaches focus on a specific uncertainty region and exploit some different objective functions to optimize. Actually, to the authors best knowledge, the problem of Maximum Likelihood (ML) joint estimation of signal amplitude and steering direction under a general steering uncertainty region, represented by a quadratic inequality constraint, has not yet been solved. To this end, in this paper, we consider steering direction ML estimation under a general quadratic inequality constraint (either convex or non-convex) and the unit norm constraint which characterizes a direction vector. We focus on two distinct situations. One assumes that complex amplitude of the received useful signal changes from snapshot to snapshot, whereas the other accounts for a constant signal amplitude in all the received snapshots. Both the situations are of interest for radar signal processing applications concerning detection of range-spread targets [13], [14], Multiple Input Multiple Output (MIMO) target detection [15], [16], and radar detection using a general antenna array configuration with a mix of high- and low-gain beams [17]. We show that, upon concentration of the likelihood function over the amplitudes of the signal of interest,

the steering direction estimation problem can be formulated as a fractional Quadratically Constrained Quadratic Problem (QCQP). Hence, in order to solve it, we first relax the problem into a constrained fractional Semidefinite Programming (SDP) which is proved equivalent to an SDP through the Charnes-Cooper transformation [18]. Then, we show that the relaxation is tight. Precisely, exploiting a suitable rank-one decomposition theorem [19], [20], we devise a technique aimed at recovering a solution of the original fractional QCQP from a solution of the fractional SDP relaxation. The overall procedure involves a polynomial computational complexity and, from the optimization theory point of view, this paper provides an efficient procedure to solve a general fractional QCQP with three homogeneous constraints, incorporating the specific rank-one decomposition technique [19].

We also provide considerations concerning the identifiability of the parameters in the considered estimation problem and evaluate the constrained Cramer Rao lower Bound (CRB) [21]. Finally, we apply the estimation framework to two radar detection problems. The former refers to radar detection of distributed targets; the latter to point-target detection with a radar using a a general antenna array configuration with a mix of high- and low-gain beams. The analysis of the resulting decision rules in comparison with the classic one, assuming aligned nominal and actual steering directions, confirms the effectiveness of the approach.

The paper is organized as follows. In Section II, we formulate the steering direction estimation problem. In Section III, we discuss the identifiability of the model parameters and propose the new estimation procedure. Additionally, we derive the constrained CRB and assess, through an example, the quality of the estimates by the proposed algorithm. In Section IV, we apply the new estimation technique to two radar problems and analyze the performance of the receivers exploiting the robust estimator of the steering direction in place of the nominal one. Finally, conclusions and possible future research tracks are given in Section V.

A. Notation

We adopt the notation of using boldface for vectors $\boldsymbol{a}$ (lower case), and matrices $\boldsymbol{A}$ (upper case). The transpose and the conjugate transpose operators are denoted by the symbols $(\cdot)^T$ and $(\cdot)^\dagger$ respectively. tr$(\cdot)$, det$(\cdot)$, rank$(\cdot)$, $\lambda_{\min}(\cdot)$, and $\lambda_{\max}(\cdot)$ are respectively the trace, the determinant, the rank, the minimum eigenvalue and the maximum eigenvalue of the square matrix argument. $\boldsymbol{I}$ and $\mathbf{0}$ denote respectively the identity matrix and the matrix with zero entries (their size is determined from the context). $\mathbb{R}^N$, $\mathbb{C}^N$, and $\mathbb{H}^N$ are respectively the sets of N-dimensional vectors of real numbers, N-dimensional vectors of complex numbers, and $N \times N$ Hermitian matrices. The curled inequality symbol $\succeq$ (and its strict form

$\succ$) is used to denote generalized matrix inequality: for any $\boldsymbol{A} \in \mathbb{H}^N$, $\boldsymbol{A} \succeq \boldsymbol{0}$ means that $\boldsymbol{A}$ is a positive semidefinite matrix ($\boldsymbol{A} \succ \boldsymbol{0}$ for positive definiteness). The Euclidean norm of the vector $\boldsymbol{x}$ is denoted by $\|\boldsymbol{x}\|$. The letter j represents the imaginary unit (i.e. $j = \sqrt{-1}$), while the letter i often serves as index in this paper. For any complex number x, we use $\Re(x)$ and $\Im(x)$ to denote respectively the real and the imaginary part of x, $|x|$ is the modulus of x, and x^* is the conjugate of x. Finally, $\otimes$ denotes the Kronecker product and for any optimization problem $\mathcal{P}$, $v(\mathcal{P})$ represents its optimal value.

II. Maximum Likelihood Steering Estimation: Problem Formulation

We assume that data are collected from N sensors (for instance the receiving elements of an antenna array) and denote by $\boldsymbol{z}_t$, $t = 1, \ldots, M$, the complex vectors of the received samples which can be expressed as

$$\boldsymbol{z}_t = \alpha_t \boldsymbol{p} + \boldsymbol{w}_t\,, \qquad t = 1, \ldots M\,, \tag{1}$$

where α_t's are unknown complex parameters accounting for the channel propagation and signal strength, $\boldsymbol{p}$ is the unit-norm steering vector of the signal of interest (i.e. $\boldsymbol{p} \in \mathcal{U}$, with $\mathcal{U} = \left\{\boldsymbol{p} \in \mathbb{C}^N : \|\boldsymbol{p}\|^2 = 1\right\}$), and $\boldsymbol{w}_t$'s are the disturbance components, modeled as statistically independent zero-mean complex circular Gaussian vectors with positive definite covariance matrix $E[\boldsymbol{w}_t \boldsymbol{w}_t^\dagger] = \boldsymbol{M}$. As to the $\alpha_t's$, we consider the following two different scenarios:

1) **Scenario 1.** It models $(\alpha_1, \ldots, \alpha_M)$ as a vector of $\mathbb{C}^M$ and is of relevant interest for radar detection of range-spread targets [13], [14], where the useful target might be spread in more than one range cell. In this case, α_t accounts for the backscattering coefficient of the scattering center in the t-th range cell (if a high resolution radar is considered) or the radar cross section from the target in the t-th range bin with reference to a formation of targets to be detected with a low-medium resolution radar.
2) **Scenario 2.** It assumes $\alpha_t = \alpha\beta_t$, $t = 1, \ldots, M$, with β_t known complex numbers, while $\alpha \in \mathbb{C}$ is an unknown parameter. This signal model is useful in MIMO radar with colocated antennas [16, p. 11, eq. 1.29] and in modern radar systems [17] that have general antenna array configurations, containing a mix of high- and low-gain beams.

Additionally, we force $\boldsymbol{p}$ to comply with a general (not necessarily convex) quadratic constraint, i.e.

$$\boldsymbol{p} \in \Omega = \mathcal{U} \cap \mathcal{C}, \;\; \text{with } \mathcal{C} = \left\{\boldsymbol{p} \in \mathbb{C}^N : \boldsymbol{p}^\dagger \boldsymbol{A} \boldsymbol{p} + 2\Re(\boldsymbol{b}^\dagger \boldsymbol{p}) + c \geq 0\right\}, \tag{2}$$

with $\boldsymbol{A} \in \mathbb{H}^N$, $\boldsymbol{b} \in \mathbb{C}^N$, and $c \in \mathbb{R}$.

The estimation of the steering direction is performed resorting to the Maximum Likelihood (ML) criterion. This technique is usually applied for radar detection applications in the presence of steering vector mismatches and/or when rejection capabilities (namely the possibility to reject signals which are outside an acceptance region centered around the expected steering direction) are required to the radar receiver[1]. Otherwise stated, we are faced with the following optimization problem:

$$\begin{array}{l} \underset{(\alpha_1,\ldots,\alpha_M)\in\mathbb{C}^M}{\text{maximize}} \ \underset{\boldsymbol{p}\in\Omega}{\text{maximize}}\ f(\boldsymbol{z}_1,\ldots,\boldsymbol{z}_M|\alpha_1,\ldots,\alpha_M,\boldsymbol{p};\boldsymbol{M})\,, \quad \text{Scenario 1} \\ \\ \underset{\alpha\in\mathbb{C}}{\text{maximize}} \ \underset{\boldsymbol{p}\in\Omega}{\text{maximize}}\ f(\boldsymbol{z}_1,\ldots,\boldsymbol{z}_M|\alpha,\boldsymbol{p};\beta_1,\ldots,\beta_M,\boldsymbol{M})\,, \quad \text{Scenario 2} \end{array} \tag{3}$$

where $f(\boldsymbol{z}_1,\ldots,\boldsymbol{z}_M|\alpha_1,\ldots,\alpha_M,\boldsymbol{p};\boldsymbol{M})$ and $f(\boldsymbol{z}_1,\ldots,\boldsymbol{z}_M|\alpha,\boldsymbol{p};\beta_1,\ldots,\beta_M,\boldsymbol{M})$ are the joint probability density functions (pdf's) of the vectors $\boldsymbol{z}_1,\ldots,\boldsymbol{z}_M$ under Scenario 1 and Scenario 2 respectively.

Exploiting the Gaussian assumption, the pdf for Scenario 1 can be written as

$$f(\boldsymbol{z}_1,\ldots,\boldsymbol{z}_M|\alpha_1,\ldots,\alpha_M,\boldsymbol{p};\boldsymbol{M}) = \frac{1}{\pi^{NM}\det^M(\boldsymbol{M})}\exp\left[-\sum_{t=1}^{M}(\boldsymbol{z}_t-\alpha_t\boldsymbol{p})^\dagger\boldsymbol{M}^{-1}(\boldsymbol{z}_t-\alpha_t\boldsymbol{p})\right]\,, \tag{4}$$

whereas that for Scenario 2, it is given by

$$f(\boldsymbol{z}_1,\ldots,\boldsymbol{z}_M|\alpha,\boldsymbol{p};\beta_1,\ldots,\beta_M,\boldsymbol{M}) = \frac{1}{\pi^{NM}\det^M(\boldsymbol{M})}\exp\left[-\sum_{t=1}^{M}(\boldsymbol{z}_t-\alpha\beta_t\boldsymbol{p})^\dagger\boldsymbol{M}^{-1}(\boldsymbol{z}_t-\alpha\beta_t\boldsymbol{p})\right]\,. \tag{5}$$

This implies that the ML estimation problem can be written as

$$\mathcal{P}_{ML}\begin{cases} \underset{(\alpha_1,\ldots,\alpha_M)\in\mathbb{C}^M}{\text{minimize}} \ \underset{\boldsymbol{p}\in\Omega}{\text{minimize}}\ \displaystyle\sum_{t=1}^{M}(\boldsymbol{z}_t-\alpha_t\boldsymbol{p})^\dagger\boldsymbol{M}^{-1}(\boldsymbol{z}_t-\alpha_t\boldsymbol{p})\,, & \text{Scenario 1} \\ \\ \underset{\alpha\in\mathbb{C}}{\text{minimize}} \ \underset{\boldsymbol{p}\in\Omega}{\text{minimize}}\ \displaystyle\sum_{t=1}^{M}(\boldsymbol{z}_t-\alpha\beta_t\boldsymbol{p})^\dagger\boldsymbol{M}^{-1}(\boldsymbol{z}_t-\alpha\beta_t\boldsymbol{p})\,, & \text{Scenario 2} \end{cases} . \tag{6}$$

Before presenting the solution method to the above problems, it is necessary to highlight their practical importance and its relation to other existing methods. In radar detection, typical quadratic constraints that the vector $\boldsymbol{p}$ has to comply with are

- Conic Constraint: $\mathcal{C} = \left\{\boldsymbol{p}\in\mathbb{C}^N : |\boldsymbol{p}^\dagger\boldsymbol{p}_0|^2 \geq \gamma\|\boldsymbol{p}\|^2\right\}$, where $\boldsymbol{p}_0$ is the nominal steering vector (assumed with unit norm) and $0\leq\gamma\leq 1$. This is tantamount to limiting the minimum squared cosine angle between the actual and the nominal steering directions, namely $\boldsymbol{p}$ has to lie in a conic

[1]The joint application of the ML criterion and the optimization theory to communications problems can be found in [22], [23], [24].

region with axis $\boldsymbol{p}_0$ and whose aperture is ruled by γ. This kind of constraint is encountered in [6], [7], [8], [10], [12]. A pictorial representation of the constraint set Ω is given in Figure 1a.

- Elliptical Constraint: $\mathcal{C} = \left\{\boldsymbol{p} \in \mathbb{C}^N : (\boldsymbol{p}-\boldsymbol{p}_0)^\dagger \boldsymbol{E}(\boldsymbol{p}-\boldsymbol{p}_0) \leq 1\right\}$, where $\boldsymbol{E}$ is a positive semidefinite matrix such that $\lambda_{\max}(\boldsymbol{E}) > 1/4$.[2] This is equivalent to assuming that $\boldsymbol{p}$ lies into an ellipsoid whose center is the unit norm vector $\boldsymbol{p}_0$ and whose shape is ruled by the matrix $\boldsymbol{E}$. This constraint is commonly encountered in robust beamforming applications [2], [3], [5] and, for $\boldsymbol{E} = \frac{1}{\epsilon}\boldsymbol{I}$, it reduces to the similarity constraint $\|\boldsymbol{p}-\boldsymbol{p}_0\|^2 \leq \epsilon$ [3], [4], [25], where $0 \leq \epsilon \leq 2$ rules the size of the similarity region. A pictorial representation of the resulting constraint set Ω is given in Figure 1b. Finally, in [26], some interesting procedures to determine the uncertainty ellipsoid are proposed and discussed.
- Exterior Conic Constraint: $\mathcal{C} = \left\{\boldsymbol{p} \in \mathbb{C}^N : |\boldsymbol{p}^\dagger \boldsymbol{p}_0|^2 \leq \gamma \|\boldsymbol{p}\|^2\right\}$, namely the useful signal lies outside a conic region whose axis is the vector $\boldsymbol{p}_0$. This constraint is of relevance in radar detection problems where rejection capabilities must be conferred to the receiver [27], [9], [28]. Specifically, it arises when it becomes necessary to discriminate between a useful signal lying in a conic region (H_1 hypothesis) and an interfering signal lying in the complement of the quoted region, namely the exterior of the cone (null hypothesis H_0). The graphic representation of the constraint Ω for this specific situation is given in Figure 1c.
- Exterior Elliptical Constraint: $\mathcal{C} = \left\{\boldsymbol{p} \in \mathbb{C}^N : (\boldsymbol{p}-\boldsymbol{p}_0)^\dagger \boldsymbol{E}(\boldsymbol{p}-\boldsymbol{p}_0) \geq 1\right\}$, $\lambda_{\max}(\boldsymbol{E}) \geq 1/4$, [3] namely the useful signal has to lie outside of an ellipsoid whose center is the vector $\boldsymbol{p}_0$ (see Figure 1d for the corresponding representation of Ω).

Evidently, the aforementioned four classes of quadratic constraints may or may not be convex, and the feasible regions are non-convex, since they consist of one of the four classes of quadratic constraints and the norm constraint $||\boldsymbol{p}|| = 1$. Furthermore, the objective function of problem $\mathcal{P}_{ML}$ is neither convex nor quadratic. In fact, consider the simplest case: $M = 1$, and the objective function (for Scenario 1) becomes

$$(\boldsymbol{z}_1 - \alpha_1 \boldsymbol{p})^\dagger \boldsymbol{M}^{-1} (\boldsymbol{z}_1 - \alpha_1 \boldsymbol{p})$$

[2]Otherwise $\Omega = \mathcal{U} \cap \mathcal{C}$ reduces to $\mathcal{U}$. Indeed, suppose that $\lambda_{\max}(\boldsymbol{E}) \leq 1/4$ and $||\boldsymbol{p}|| = 1$. Then $1/4 \geq \lambda_{\max}(\boldsymbol{E}) \geq (\boldsymbol{p}-\boldsymbol{p}_0)^\dagger \boldsymbol{E}(\boldsymbol{p}-\boldsymbol{p}_0)/||\boldsymbol{p}-\boldsymbol{p}_0||^2 \geq (\boldsymbol{p}-\boldsymbol{p}_0)^\dagger \boldsymbol{E}(\boldsymbol{p}-\boldsymbol{p}_0)/(||\boldsymbol{p}|| + ||\boldsymbol{p}_0||)^2 = (\boldsymbol{p}-\boldsymbol{p}_0)^\dagger \boldsymbol{E}(\boldsymbol{p}-\boldsymbol{p}_0)/4$, which implies $(\boldsymbol{p}-\boldsymbol{p}_0)^\dagger \boldsymbol{E}(\boldsymbol{p}-\boldsymbol{p}_0) \leq 1$; in other words, $\lambda_{\max}(\boldsymbol{E}) \leq 1/4$ and $||\boldsymbol{p}|| = 1$ imply $\boldsymbol{p} \in \mathcal{C}$.

[3]Otherwise, the set $\Omega = \mathcal{U} \cap \mathcal{C}$ is empty. Indeed, suppose that $\lambda_{\max}(\boldsymbol{E}) < 1/4$, $\boldsymbol{p} \in \mathcal{C}$ and $||\boldsymbol{p}|| = 1$, and then one gets the contradiction: $1/4 > \lambda_{\max}(\boldsymbol{E}) \geq \frac{(\boldsymbol{p}-\boldsymbol{p}_0)^\dagger \boldsymbol{E}(\boldsymbol{p}-\boldsymbol{p}_0)}{||\boldsymbol{p}-\boldsymbol{p}_0||^2} \geq \frac{(\boldsymbol{p}-\boldsymbol{p}_0)^\dagger \boldsymbol{E}(\boldsymbol{p}-\boldsymbol{p}_0)}{(||\boldsymbol{p}||+||\boldsymbol{p}_0||)^2} \geq 1/4$.

(set $\beta_t = 1$ for Scenario 2). Evaluating the Hessian matrix

$$\begin{bmatrix} |\alpha_1|^2 \boldsymbol{M}^{-1} & \alpha_1 \boldsymbol{M}^{-1}\boldsymbol{p} - \boldsymbol{M}^{-1}\boldsymbol{z}_1 \\ \alpha_1^\dagger \boldsymbol{p}^\dagger \boldsymbol{M}^{-1} - \boldsymbol{z}_1^\dagger \boldsymbol{M}^{-1} & \boldsymbol{p}^\dagger \boldsymbol{M}^{-1}\boldsymbol{p} \end{bmatrix}, \tag{7}$$

it is neither a constant matrix nor a positive semidefinite matrix for some $(\boldsymbol{p}, \alpha) \in \Omega \times \mathbb{C}$.[4] In other words, the objective function is neither quadratic nor convex; thus problem $\mathcal{P}_{ML}$ is a non-convex program (neither a QCQP), and seems difficult to solve. However, we will show that the problem can be solved efficiently. Precisely, in the next section, we will show that problem $\mathcal{P}_{ML}$, after concentration over the complex amplitudes α_t's for Scenario 1 (over α for Scenario 2) is equivalent to a fractional SDP, whose solutions can be obtained by solving its equivalent SDP via the so-called Charnes-Cooper transformation [18]. Then, we retrieve an optimal solution of $\mathcal{P}_{ML}$ from an optimal solution to the equivalent fractional SDP through specific rank-one decompositions [19].

III. Identifiability, Solution to the ML Steering Direction Estimation Problem, and Constrained CRB

In this section, we first address the identifiability of the model parameters, then we introduce the new algorithm which in polynomial time provides a solution to the estimation problem, and, finally, we assess the quality of the derived estimate through a comparison with the constrained CRB for the considered problem.

A. Identifiability of the Model Parameters

Identifiability refers to the study of the solution to the estimation problem in the noiseless case. It is basically a consistency aspect which allows to understand whether the solution is unique in the ideal case of no noise. With reference to our problem, the identifiability equations can be written as

$$\alpha_t \boldsymbol{p} = \check{\alpha}_t \check{\boldsymbol{p}}, \qquad t = 1, \ldots, M, \qquad \text{Scenario 1} \tag{8}$$

($\alpha \boldsymbol{p} = \check{\alpha}\check{\boldsymbol{p}}$ for Scenario 2). Assuming that $\check{\boldsymbol{p}} \in \Omega$ and $\check{\alpha}_t$'s ($\check{\alpha}$ for Scenario 2) are complex numbers, the identifiability of the parameters α_t, $t = 1, \ldots, M$, and $\boldsymbol{p}$ holds if (8) has a unique solution with $\boldsymbol{p} \in \Omega$. Evidently this is not the case since both $\check{\alpha}_t$'s ($\check{\alpha}$ for Scenario 2) $\check{\boldsymbol{p}}$ and $\check{\alpha}_t e^{j\phi_g}$'s ($\check{\alpha} e^{j\phi_g}$ for Scenario 2)

[4]For example, at the points $(0, \boldsymbol{p})$, $(\alpha_1, \boldsymbol{0})$, $(0, \boldsymbol{0})$, the Hessian matrix (7) is not positive semidefinite.

$\check{\boldsymbol{p}}e^{-j\phi_g}$ with

$$\phi_g = \begin{cases} \arg(\boldsymbol{b}^\dagger \check{\boldsymbol{p}}) & \text{if } \boldsymbol{b} \neq \mathbf{0} \\ \\ \arg(\mathbf{e}_1 \check{\boldsymbol{p}}) & \text{if } \boldsymbol{b} = \mathbf{0} \end{cases}$$

(where $\boldsymbol{b}$ is defined in (2)) and $\mathbf{e}_1 = [1, 0, \ldots, 0]^T$, are solutions of equation (8). Nevertheless, we can easily obtain identifiability imposing a further constraint on $\boldsymbol{p}$, i.e.

$$\begin{aligned} &\Im(\boldsymbol{b}^\dagger \boldsymbol{p}) = 0\,, \qquad \Re(\boldsymbol{b}^\dagger \boldsymbol{p}) \geq 0 \qquad \text{if } \boldsymbol{b} \neq 0\,, \\ &\Im(\mathbf{e}_1^\dagger \boldsymbol{p}) = 0\,, \qquad \Re(\mathbf{e}_1^\dagger \boldsymbol{p}) \geq 0 \qquad \text{if } \boldsymbol{b} = 0\,. \end{aligned} \tag{9}$$

With this additional constraint the phase ambiguity is eliminated and the solution of (8) is unique thanks to the unit norm condition.

It is worth pointing out that if the last constraint (9) is added to the estimation problem of Section II, the algorithm, we will propose in the next subsection, can be still applied to obtain the ML estimates of the parameters provided that its output $(\alpha_{1_{ML}}, \ldots, \alpha_{M_{ML}}, \boldsymbol{p}_{ML})$ ($(\alpha_{_{ML}}, \boldsymbol{p}_{ML})$ for Scenario 2) is phase rotated in order to comply with (9). In the following, the set Ω augmented with (9) is denoted by Ω_a.

B. Solution to the ML Steering Direction Estimation Problem

In this subsection, we show how the solution to the ML steering estimation problem can be obtained in polynomial time. To this end, we observe that problem $\mathcal{P}_{_{ML}}$ can be equivalently rewritten as

$$\mathcal{P} \begin{cases} \underset{\boldsymbol{p} \in \Omega}{\text{minimize}} \displaystyle\sum_{t=1}^{M} \underset{\alpha_t \in \mathbb{C}}{\text{minimize}} (\boldsymbol{z}_t - \alpha_t \boldsymbol{p})^\dagger \boldsymbol{M}^{-1} (\boldsymbol{z}_t - \alpha_t \boldsymbol{p})\,, & \text{Scenario 1} \\ \\ \underset{\boldsymbol{p} \in \Omega}{\text{minimize}} \; \underset{\alpha \in \mathbb{C}}{\text{minimize}} \displaystyle\sum_{t=1}^{M} (\boldsymbol{z}_t - \alpha \beta_t \boldsymbol{p})^\dagger \boldsymbol{M}^{-1} (\boldsymbol{z}_t - \alpha \beta_t \boldsymbol{p})\,, & \text{Scenario 2} \end{cases} \tag{10}$$

The inner minimization is direct, i.e. for Scenario 1

$$-\frac{\boldsymbol{p}^\dagger \boldsymbol{M}^{-1} \boldsymbol{z}_t \boldsymbol{z}_t^\dagger \boldsymbol{M}^{-1} \boldsymbol{p}}{\boldsymbol{p}^\dagger \boldsymbol{M}^{-1} \boldsymbol{p}} + \boldsymbol{z}_t^\dagger \boldsymbol{M}^{-1} \boldsymbol{z}_t = \underset{\alpha_t \in \mathbb{C}}{\text{minimize}} (\boldsymbol{z}_t - \alpha_t \boldsymbol{p})^\dagger \boldsymbol{M}^{-1} (\boldsymbol{z}_t - \alpha_t \boldsymbol{p}), \tag{11}$$

and the minimal value is attained at

$$\alpha_t^\star = \frac{\boldsymbol{p}^\dagger \boldsymbol{M}^{-1} \boldsymbol{z}_t}{\boldsymbol{p}^\dagger \boldsymbol{M}^{-1} \boldsymbol{p}}\,. \tag{12}$$

For Scenario 2,

$$-\frac{\boldsymbol{p}^\dagger \boldsymbol{M}^{-1} \boldsymbol{q} \boldsymbol{q}^\dagger \boldsymbol{M}^{-1} \boldsymbol{p}}{\boldsymbol{p}^\dagger \boldsymbol{M}^{-1} \boldsymbol{p}} + \sum_{t=1}^{M} \boldsymbol{z}_t^\dagger \boldsymbol{M}^{-1} \boldsymbol{z}_t = \underset{\alpha \in \mathbb{C}}{\text{minimize}} \sum_{t=1}^{M} (\boldsymbol{z}_t - \alpha \beta_t \boldsymbol{p})^\dagger \boldsymbol{M}^{-1} (\boldsymbol{z}_t - \alpha \beta_t \boldsymbol{p}), \tag{13}$$

with

$$\boldsymbol{q} = \frac{\sum_{t=1}^{M} \beta_t^{\dagger} \boldsymbol{z}_t}{\sqrt{\sum_{t=1}^{M} |\beta_t|^2}},$$

and the minimal value is attained at

$$\alpha_t^{\star} = \frac{\sum_{t=1}^{M} \beta_t^{\dagger} \boldsymbol{p}^{\dagger} \boldsymbol{M}^{-1} \boldsymbol{z}_t}{\sum_{t=1}^{M} |\beta_t|^2 \boldsymbol{p}^{\dagger} \boldsymbol{M}^{-1} \boldsymbol{p}} = \frac{\boldsymbol{p}^{\dagger} \boldsymbol{M}^{-1} \boldsymbol{q}}{\boldsymbol{p}^{\dagger} \boldsymbol{M}^{-1} \boldsymbol{p} \sqrt{\sum_{t=1}^{M} |\beta_t|^2}}. \tag{14}$$

Therefore, $\mathcal{P}$ amounts to

$$\sum_{t=1}^{M} \boldsymbol{z}_t^{\dagger} \boldsymbol{M}^{-1} \boldsymbol{z}_t + \underset{\boldsymbol{p} \in \Omega}{\mathsf{minimize}} - \frac{\boldsymbol{p}^{\dagger} \boldsymbol{M}^{-1} \boldsymbol{S} \boldsymbol{M}^{-1} \boldsymbol{p}}{\boldsymbol{p}^{\dagger} \boldsymbol{M}^{-1} \boldsymbol{p}} = \sum_{t=1}^{M} \boldsymbol{z}_t^{\dagger} \boldsymbol{M}^{-1} \boldsymbol{z}_t - \underset{\boldsymbol{p} \in \Omega}{\mathsf{maximize}} \frac{\boldsymbol{p}^{\dagger} \boldsymbol{M}^{-1} \boldsymbol{S} \boldsymbol{M}^{-1} \boldsymbol{p}}{\boldsymbol{p}^{\dagger} \boldsymbol{M}^{-1} \boldsymbol{p}}, \tag{15}$$

where

$$\boldsymbol{S} = \begin{cases} \sum_{t=1}^{M} \boldsymbol{z}_t \boldsymbol{z}_t^{\dagger}, & \text{Scenario 1} \\ \boldsymbol{q} \boldsymbol{q}^{\dagger}, & \text{Scenario 2} \end{cases} \tag{16}$$

Now, let us focus on solving the fractional QCQP

$$\mathcal{P}_1 \quad \begin{cases} \underset{\boldsymbol{p} \in \Omega}{\mathsf{maximize}} \ \dfrac{\boldsymbol{p}^{\dagger} \boldsymbol{M}^{-1} \boldsymbol{S} \boldsymbol{M}^{-1} \boldsymbol{p}}{\boldsymbol{p}^{\dagger} \boldsymbol{M}^{-1} \boldsymbol{p}}, \end{cases} \tag{17}$$

where Ω is defined by (2). The homogenized version of $\mathcal{P}_1$ is

$$\mathcal{P}_2 \begin{cases} \underset{\boldsymbol{p},\, t}{\mathsf{maximize}} & \dfrac{\mathrm{tr}\left(\begin{bmatrix} \boldsymbol{M}^{-1} \boldsymbol{S}^{\dagger} \boldsymbol{M}^{-1} & \boldsymbol{0} \\ \boldsymbol{0} & 0 \end{bmatrix} \begin{bmatrix} \boldsymbol{p}\boldsymbol{p}^{\dagger} & \boldsymbol{p} t^{*} \\ \boldsymbol{p}^{\dagger} t & |t|^2 \end{bmatrix} \right)}{\mathrm{tr}\left(\begin{bmatrix} \boldsymbol{M}^{-1} & \boldsymbol{0} \\ \boldsymbol{0} & 0 \end{bmatrix} \begin{bmatrix} \boldsymbol{p}\boldsymbol{p}^{\dagger} & \boldsymbol{p} t^{*} \\ \boldsymbol{p}^{\dagger} t & |t|^2 \end{bmatrix} \right)} \\ \mathsf{subject\ to} & \mathrm{tr}\left(\begin{bmatrix} \boldsymbol{A} & \boldsymbol{b} \\ \boldsymbol{b}^{\dagger} & c \end{bmatrix} \begin{bmatrix} \boldsymbol{p}\boldsymbol{p}^{\dagger} & \boldsymbol{p} t^{*} \\ \boldsymbol{p}^{\dagger} t & |t|^2 \end{bmatrix} \right) \geq 0 \\ & \mathrm{tr}\left(\begin{bmatrix} \boldsymbol{I} & \boldsymbol{0} \\ \boldsymbol{0} & 0 \end{bmatrix} \begin{bmatrix} \boldsymbol{p}\boldsymbol{p}^{\dagger} & \boldsymbol{p} t^{*} \\ \boldsymbol{p}^{\dagger} t & |t|^2 \end{bmatrix} \right) = 1 \\ & \mathrm{tr}\left(\begin{bmatrix} \boldsymbol{0} & \boldsymbol{0} \\ \boldsymbol{0} & 1 \end{bmatrix} \begin{bmatrix} \boldsymbol{p}\boldsymbol{p}^{\dagger} & \boldsymbol{p} t^{*} \\ \boldsymbol{p}^{\dagger} t & |t|^2 \end{bmatrix} \right) = 1 \\ & \boldsymbol{p} \in \mathbb{C}^N,\ t \in \mathbb{C}. \end{cases} \tag{18}$$

We highlight that the two problems $\mathcal{P}_1$ and $\mathcal{P}_2$ have the same optimal value (i.e. $v(\mathcal{P}_1) = v(\mathcal{P}_2)$), and $\boldsymbol{p}^{\star}/t^{\star}$ is optimal to $\mathcal{P}_1$ if $(\boldsymbol{p}^{\star},\, t^{\star})$ solves $\mathcal{P}_2$. In fact, it is evident that $v(\mathcal{P}_1) \leq v(\mathcal{P}_2)$; on the other hand, the objective function of $\mathcal{P}_1$ evaluated at $\boldsymbol{p}^{\star}/t^{\star}$ is equal to the optimal value of $\mathcal{P}_2$, provided that $(\boldsymbol{p}^{\star}, t^{\star})$ is an optimal solution for $\mathcal{P}_2$.

The SDP relaxation of $\mathcal{P}_2$ is:

$$\mathcal{P}_3 \begin{cases} \underset{\boldsymbol{W}}{\text{maximize}} & \frac{\text{tr}(\boldsymbol{Q}_{-1}\boldsymbol{W})}{\text{tr}(\boldsymbol{Q}_{0}\boldsymbol{W})} \\ \text{subject to} & \text{tr}\left(\boldsymbol{Q}_1\boldsymbol{W}\right) \geq 0 \\ & \text{tr}\left(\boldsymbol{Q}_2\boldsymbol{W}\right) = 1 \\ & \text{tr}\left(\boldsymbol{Q}_3\boldsymbol{W}\right) = 1 \\ & \boldsymbol{W} \succeq \boldsymbol{0}, \end{cases} \tag{19}$$

where $\boldsymbol{Q}_i$'s, are defined as follows:

$$\boldsymbol{Q}_{-1} = \begin{bmatrix} \boldsymbol{M}^{-1}\boldsymbol{S}\boldsymbol{M}^{-1} & \boldsymbol{0} \\ \boldsymbol{0} & 0 \end{bmatrix}, \boldsymbol{Q}_0 = \begin{bmatrix} \boldsymbol{M}^{-1} & \boldsymbol{0} \\ \boldsymbol{0} & 0 \end{bmatrix}, \tag{20}$$

and

$$\boldsymbol{Q}_1 = \begin{bmatrix} \boldsymbol{A} & \boldsymbol{b} \\ \boldsymbol{b}^\dagger & c \end{bmatrix}, \boldsymbol{Q}_2 = \begin{bmatrix} \boldsymbol{I} & \boldsymbol{0} \\ \boldsymbol{0} & 0 \end{bmatrix}, \boldsymbol{Q}_3 = \begin{bmatrix} \boldsymbol{0} & \boldsymbol{0} \\ \boldsymbol{0} & 1 \end{bmatrix}. \tag{21}$$

It is known that the single-ratio fractional SDP $\mathcal{P}_3$ can be iteratively solved by either the Dinkelbach algorithm (for instance see [29], [30]) or the bisection search (see [31]). In this paper, we will solve $\mathcal{P}_3$ in one single shot by resorting to a variation of the so-called Charnes-Cooper variable transformation which was originally introduced in [18]. By the Charnes-Cooper variable transformation, one can replace a linear fractional program with at most two straightforward linear programs that differ from each other by only a change of sign in the objective function and in one constraint, and thus achieves a global optimal solution of the linear fractional program by solving at most two linear programs. By using the idea of Charnes and Cooper's transformation, and considering that the denominator of the fractional SDP $\mathcal{P}_3$ is always positive, we can convert the fractional SDP into an equivalent SDP. Precisely, let us define the transformed variable $\boldsymbol{X} = s\boldsymbol{W}$, where $s \geq 0$ complies with $\text{tr}(\boldsymbol{Q}_0(s\boldsymbol{W})) = 1$. Hence, multiplying by s the numerator and the denominator of the objective function in $\mathcal{P}_3$, we come up with the SDP problem

$$\mathcal{P}_4 \begin{cases} \underset{\boldsymbol{X},\ s}{\text{maximize}} & \text{tr}\left(\boldsymbol{Q}_{-1}\boldsymbol{X}\right) \\ \text{subject to} & \text{tr}\left(\boldsymbol{Q}_0\boldsymbol{X}\right) = 1 \\ & \text{tr}\left(\boldsymbol{Q}_1\boldsymbol{X}\right) \geq 0 \\ & \text{tr}\left(\boldsymbol{Q}_2\boldsymbol{X}\right) = s \\ & \text{tr}\left(\boldsymbol{Q}_3\boldsymbol{X}\right) = s \\ & \boldsymbol{X} \succeq \boldsymbol{0},\ s \geq 0. \end{cases} \tag{22}$$

In the following, we show that the fractional SDP $\mathcal{P}_3$ is equivalent to the SDP (22), in the sense that they have the equal optimal value and optimal solutions differ from one to another by a constant. In order to

claim the equivalence between $\mathcal{P}_3$ and $\mathcal{P}_4$, we first prove three lemmas showing that the two problems are solvable [5] (Lemmas 3.1 and 3.2), and that they share the same optimal value (Lemma 3.3) even if the optimal solutions differ up to a scalar whose expression is specified in Lemma 3.3.

Lemma 3.1: The fractional SDP problem $\mathcal{P}_3$ is solvable.

Proof: See Appendix A. ■

Lemma 3.2: The SDP problem $\mathcal{P}_4$ is solvable.

Proof: See Appendix B. ■

Lemma 3.3: Problems $\mathcal{P}_3$ and $\mathcal{P}_4$ have the equal optimal value. Furthermore, if $\boldsymbol{X}^\star$ solves $\mathcal{P}_3$, then $(\boldsymbol{X}^\star/\text{tr}(\boldsymbol{Q}_0\boldsymbol{X}^\star),\, 1/\text{tr}(\boldsymbol{Q}_0\boldsymbol{X}^\star))$ solves $\mathcal{P}_4$; if $(\boldsymbol{X}^\star,\, s^\star)$ solves $\mathcal{P}_4$, then $\boldsymbol{X}^\star/s^\star$ solves $\mathcal{P}_3$.

Proof: See Appendix C. ■

Once an optimal solution $\boldsymbol{X}^\star$ of $\mathcal{P}_3$ is obtained, we can check the rank of $\boldsymbol{X}^\star$. If $\boldsymbol{X}^\star$ is of rank one, then the solution is a global optimal solution of the fractional QCQP $\mathcal{P}_2$ since $\mathcal{P}_3$ is a relaxation of $\mathcal{P}_2$ by dropping the rank-one constraint. If $\boldsymbol{X}^\star$ is of rank higher than one, we will construct a rank-one optimal solution $\boldsymbol{x}^\star(\boldsymbol{x}^\star)^\dagger$ of $\mathcal{P}_3$ by a recent matrix decomposition theorem [19]. Then, the solution $\boldsymbol{x}^\star$ is an optimal solution of $\mathcal{P}_2$. In other words, the SDP relaxation (19) is tight. Specifically, in order to construct a rank-one optimal solution to $\mathcal{P}_3$, we use the rank-one matrix decomposition theorem [19, Theorem 2.3], which is cited as the following lemma.

Lemma 3.4: Let $\boldsymbol{X}$ be a non-zero $N \times N$ ($N \geq 3$) complex Hermitian positive semidefinite matrix and $\boldsymbol{A}_i$ be Hermitian matrix, $i = 1, 2, 3, 4$, and suppose that $(\text{tr}\,(\boldsymbol{Y}\boldsymbol{A}_1)\,, \text{tr}\,(\boldsymbol{Y}\boldsymbol{A}_2)\,, \text{tr}\,(\boldsymbol{Y}\boldsymbol{A}_3),\ \text{tr}\,(\boldsymbol{Y}\boldsymbol{A}_4)) \neq (0, 0, 0, 0)$ for any non-zero complex Hermitian positive semidefinite matrix $\boldsymbol{Y}$ of size $N \times N$. Then,

- if $\text{rank}(\boldsymbol{X}) \geq 3$, one can find, in polynomial time, a rank-one matrix $\boldsymbol{x}\boldsymbol{x}^\dagger$ such that $\boldsymbol{x}$ (synthetically denoted as $\mathcal{D}_1(\boldsymbol{X}, \boldsymbol{A}_1, \boldsymbol{A}_2, \boldsymbol{A}_3, \boldsymbol{A}_4)$) is in $\text{range}(\boldsymbol{X})$, and
$$\boldsymbol{x}^\dagger \boldsymbol{A}_i \boldsymbol{x} = \text{tr}\,(\boldsymbol{X}\boldsymbol{A}_i)\,, \quad i = 1, 2, 3, 4;$$
- if $\text{rank}(\boldsymbol{X}) = 2$, for any $\boldsymbol{z}$ not in the range space of $\boldsymbol{X}$, one can find a rank-one matrix $\boldsymbol{x}\boldsymbol{x}^\dagger$ such that $\boldsymbol{x}$ (synthetically denoted as $\mathcal{D}_2(\boldsymbol{X}, \boldsymbol{A}_1, \boldsymbol{A}_2, \boldsymbol{A}_3, \boldsymbol{A}_4)$) is in the linear subspace spanned by $\{\boldsymbol{z}\} \cup \text{range}(\boldsymbol{X})$, and
$$\boldsymbol{x}^\dagger \boldsymbol{A}_i \boldsymbol{x} = \text{tr}\,(\boldsymbol{X}\boldsymbol{A}_i)\,, \quad i = 1, 2, 3, 4.$$

Let us check the applicability of the lemma to both $\boldsymbol{X}^\star$ and the matrix parameters of $\mathcal{P}_3$. Indeed, the

[5] By "solvable," we mean that the problem is feasible and bounded, and the optimal value is attained; see [32, page 13].

condition $N \geq 3$ is mild and practical. Now, in order to verify

$$(\mathrm{tr}\,(\boldsymbol{Y}\boldsymbol{Q}_1), \mathrm{tr}\,(\boldsymbol{Y}\boldsymbol{Q}_2), \mathrm{tr}\,(\boldsymbol{Y}\boldsymbol{Q}_3), \mathrm{tr}\,(\boldsymbol{Y}\boldsymbol{Q}_4)) \neq (0,0,0,0), \text{ for any non-zero } \boldsymbol{Y} \succeq 0,$$

it suffices to prove that there is $(a_1, a_2, a_3, a_4) \in \mathbb{R}^4$ such that

$$a_1\boldsymbol{Q}_1 + a_2\boldsymbol{Q}_2 + a_3\boldsymbol{Q}_3 + a_4\boldsymbol{Q}_4 \succ 0,$$

where

$$\boldsymbol{Q}_4 = \begin{bmatrix} \boldsymbol{M}^{-1}\boldsymbol{S}\boldsymbol{M}^{-1} - v(\mathcal{P}_3)\boldsymbol{M}^{-1} & \boldsymbol{0} \\ \boldsymbol{0} & 0 \end{bmatrix}.$$

But this is evident for the matrix parameters[6] of $\mathcal{P}_2$.

Algorithm 1 summarizes the procedure leading to an optimal solution $\boldsymbol{p}^\star$ of $\mathcal{P}_1$.

Algorithm 1 : Algorithm for fractional QCQP $\mathcal{P}_1$

Input: $\boldsymbol{M}^{-1}$, $\boldsymbol{S}$, $\boldsymbol{Q}_1$.

Output: An optimal solution $\boldsymbol{p}^\star$ of $\mathcal{P}_1$.

1: solve SDP $\mathcal{P}_4$ finding an optimal solution $(\boldsymbol{X}^\star, s^\star)$ and the optimal value $v^\star$;

2: let $\boldsymbol{X}^\star := \boldsymbol{X}^\star / s^\star$;

3: **if** $\mathrm{rank}\,(\boldsymbol{X}^\star) = 1$ **then**

4: perform an eigen-decomposition $\boldsymbol{X}^\star = \boldsymbol{x}^\star(\boldsymbol{x}^\star)^\dagger$, where $\boldsymbol{x}^\star = \begin{bmatrix} \boldsymbol{p}^\star \\ t^\star \end{bmatrix}$; output $\boldsymbol{p}^\star := \boldsymbol{p}^\star / t^\star$ and terminate.

5: **else if** $\mathrm{rank}\,(\boldsymbol{X}^\star) = 2$ **then**

6: find $\boldsymbol{x}^\star = \mathcal{D}_2\left(\boldsymbol{X}^\star, \begin{bmatrix} \boldsymbol{M}^{-1}\boldsymbol{S}\boldsymbol{M}^{-1} - v^\star\boldsymbol{M}^{-1} & \boldsymbol{0} \\ \boldsymbol{0} & 0 \end{bmatrix}, \begin{bmatrix} \boldsymbol{A} & \boldsymbol{b} \\ \boldsymbol{b}^\dagger & c \end{bmatrix}, \begin{bmatrix} \boldsymbol{I} & \boldsymbol{0} \\ \boldsymbol{0} & 0 \end{bmatrix}, \begin{bmatrix} \boldsymbol{0} & \boldsymbol{0} \\ \boldsymbol{0} & 1 \end{bmatrix}\right)$;

7: **else**

8: find $\boldsymbol{x}^\star = \mathcal{D}_1\left(\boldsymbol{X}^\star, \begin{bmatrix} \boldsymbol{M}^{-1}\boldsymbol{S}\boldsymbol{M}^{-1} - v^\star\boldsymbol{M}^{-1} & \boldsymbol{0} \\ \boldsymbol{0} & 0 \end{bmatrix}, \begin{bmatrix} \boldsymbol{A} & \boldsymbol{b} \\ \boldsymbol{b}^\dagger & c \end{bmatrix}, \begin{bmatrix} \boldsymbol{I} & \boldsymbol{0} \\ \boldsymbol{0} & 0 \end{bmatrix}, \begin{bmatrix} \boldsymbol{0} & \boldsymbol{0} \\ \boldsymbol{0} & 1 \end{bmatrix}\right)$;

9: **end**

10: let $\boldsymbol{x}^\star = \begin{bmatrix} \boldsymbol{p}^\star \\ t^\star \end{bmatrix}$; output $\boldsymbol{p}^\star := \boldsymbol{p}^\star / t^\star$.

---

[6]In fact, taking $a_1 = a_2 = 0$ and $a_3 = a_4 = 1$, then $a_1\boldsymbol{Q}_1 + a_2\boldsymbol{Q}_2 + a_3\boldsymbol{Q}_3 + a_4\boldsymbol{Q}_4 = \boldsymbol{I} \succ 0$.

The computational complexity, connected with the implementation of **Algorithm 1**[7] includes the complexity of solving SDP $\mathcal{P}_4$, which is of order $O(N^{3.5}\log(1/\eta))$ (see [32, page 250]), where η is a prefixed accuracy, and the complexity of the specific rank-one decomposition procedure which is $O\left(N^3\right)$.

Given an optimal solution $\boldsymbol{p}^\star$ of $\mathcal{P}_1$, it follows by (12) that for Scenario 1, $(\alpha_1^\star,\ldots,\alpha_M^\star,\boldsymbol{p}^\star) = \left(\frac{(\boldsymbol{p}^\star)^\dagger \boldsymbol{M}^{-1}\boldsymbol{z}_1}{(\boldsymbol{p}^\star)^\dagger \boldsymbol{M}^{-1}\boldsymbol{p}^\star},\ldots,\ \frac{(\boldsymbol{p}^\star)^\dagger \boldsymbol{M}^{-1}\boldsymbol{z}_M}{(\boldsymbol{p}^\star)^\dagger \boldsymbol{M}^{-1}\boldsymbol{p}^\star},\boldsymbol{p}^\star\right)$ (for Scenario 2, $(\alpha^\star,\boldsymbol{p}^\star) = \left(\frac{(\boldsymbol{p}^\star)^\dagger \boldsymbol{M}^{-1}\boldsymbol{q}}{\sqrt{\sum_{t=1}^M |\beta_t|^2}(\boldsymbol{p}^\star)^\dagger \boldsymbol{M}^{-1}\boldsymbol{p}^\star},\boldsymbol{p}^\star\right)$) is an optimal solution of problem $\mathcal{P}_{ML}$. **Algorithm 2** describes the procedure to find the ML estimates (i.e. the optimal solution to $\mathcal{P}_{ML}$).

Algorithm 2 : Finding an optimal solution of $\mathcal{P}_{ML}$

Input: $\boldsymbol{M}^{-1}$, $\boldsymbol{z}_1,\ldots,\boldsymbol{z}_M$, $\boldsymbol{Q}_1$.

Output: An optimal solution $(\alpha_{1_{ML}},\ldots,\alpha_{M_{ML}},\boldsymbol{p}_{ML})$ for Scenario 1 ($(\alpha_{ML},\boldsymbol{p}_{ML})$ for Scenario 2).

1: define $\boldsymbol{S}$ as (16);

2: $\boldsymbol{p}^\star =$ Algorithm 1$(\boldsymbol{M},\boldsymbol{S},\boldsymbol{Q}_1,\boldsymbol{X}_0)$.

3: let $\alpha_{t_{ML}} := \frac{(\boldsymbol{p}^\star)^\dagger \boldsymbol{M}^{-1}\boldsymbol{z}_t}{(\boldsymbol{p}^\star)^\dagger \boldsymbol{M}^{-1}\boldsymbol{p}^\star}$, $t = 1,\ldots M$, and $\boldsymbol{p}_{ML} := \boldsymbol{p}^\star$ for Scenario 1 ($\alpha_{ML} := \frac{(\boldsymbol{p}^\star)^\dagger \boldsymbol{M}^{-1}\boldsymbol{q}}{\sqrt{\sum_{t=1}^M |\beta_t|^2}(\boldsymbol{p}^\star)^\dagger \boldsymbol{M}^{-1}\boldsymbol{p}^\star}$, and $\boldsymbol{p}_{ML} := \boldsymbol{p}^\star$ for Scenario 2).

C. Constrained CRB and Accuracy of the Proposed Estimator

In this subsection, we evaluate the constrained CRB for the estimation of $\boldsymbol{p}$ and analyze the quality of the estimator proposed in the previous subsection through a comparison between its accuracy and the CRB. Assuming that $\boldsymbol{p}$ is a regular point of the inequality constraints involved in Ω_a, the CRB under the constraint $\boldsymbol{p}\in\Omega_a$ is identical to that under the constraints $\boldsymbol{p}\in\mathcal{U}$ and $\Im(\boldsymbol{b}_a^\dagger\boldsymbol{p})=0$ (with $\boldsymbol{b}_a=\boldsymbol{b}$ if $\boldsymbol{b}\neq\boldsymbol{0}$ and $\boldsymbol{b}_a=\mathbf{e}_1$ otherwise) [33]. In other words, only the equality constraints have to be considered. In the following, we derive the CRB exploiting the technique proposed in [21].

Let us define $\boldsymbol{\theta}_p = [\Re(\boldsymbol{p})^T,\Im(\boldsymbol{p})^T]^T$, $\boldsymbol{\theta}_\alpha = [\Re(\alpha_1),\Im(\alpha_1),\ldots,\Re(\alpha_M),\Im(\alpha_M)]^T$ for Scenario 1 ($\boldsymbol{\theta}_\alpha = [\Re(\alpha),\Im(\alpha)]^T$ for Scenario 2), and $\boldsymbol{\theta} = [\boldsymbol{\theta}_p^T,\boldsymbol{\theta}_\alpha^T]^T$. After some standard algebra, the Fisher

[7]We highlight that **Algorithm 1** includes solving the SDP relaxation problem $\mathcal{P}_4$, performing a similar Charnes-Cooper transformation, and some matrix rank-one decompositions which are specified in Lemma 3.4. Algorithm 1 of [19] demonstrates how to decompose a positive semidefinite matrix according to Theorem 2.1 of [19]. In fact, Theorem 2.1 of [19] and Theorem 2.1 of [20] are the core of the rank-one decompositions described in Theorem 2.3 of [19] (cited by Lemma 3.4 herein).

Information Matrix (FIM) [34] $\boldsymbol{J}$ can be written as

$$\boldsymbol{J}(\boldsymbol{\theta}) = \begin{bmatrix} \boldsymbol{J}_{\boldsymbol{\theta}_p,\boldsymbol{\theta}_p}(\boldsymbol{\theta}) & \boldsymbol{J}_{\boldsymbol{\theta}_p,\boldsymbol{\theta}_\alpha}(\boldsymbol{\theta}) \\ \\ \boldsymbol{J}_{\boldsymbol{\theta}_\alpha,\boldsymbol{\theta}_p}(\boldsymbol{\theta}) & \boldsymbol{J}_{\boldsymbol{\theta}_\alpha,\boldsymbol{\theta}_\alpha}(\boldsymbol{\theta}) \end{bmatrix}$$

where

$$\boldsymbol{J}_{\boldsymbol{\theta}_p,\boldsymbol{\theta}_p}(\boldsymbol{\theta}) = 2\xi\Re\left(\begin{bmatrix} 1 & j \\ \\ -j & 1 \end{bmatrix} \otimes \boldsymbol{M}^{-1}\right),$$

with $\xi = \sum_{t=1}^{M} |\alpha_t|^2$ for Scenario 1 and $\xi = |\alpha|^2 \sum_{t=1}^{M} |\beta_t|^2$ for Scenario 2;

$$\boldsymbol{J}_{\boldsymbol{\theta}_\alpha,\boldsymbol{\theta}_\alpha}(\boldsymbol{\theta}) = \begin{cases} 2\boldsymbol{p}^\dagger \boldsymbol{M}^{-1}\boldsymbol{p}\, \boldsymbol{I}_{2M} \\ \\ 2\sum_{t=1}^{M} |\beta_t|^2 \boldsymbol{p}^\dagger \boldsymbol{M}^{-1}\boldsymbol{p}\, \boldsymbol{I}_2 \end{cases}$$

and

$$\boldsymbol{J}_{\boldsymbol{\theta}_\alpha,\boldsymbol{\theta}_p}(\boldsymbol{\theta}) = 2\Re\left(\begin{bmatrix} 1 & j \\ \\ -j & 1 \end{bmatrix} \otimes \boldsymbol{v}_\xi \otimes \boldsymbol{p}^\dagger \boldsymbol{M}^{-1}\right),$$

with $\boldsymbol{v}_\xi = [\alpha_1, \ldots, \alpha_M]^T$ for Scenario 1 and $\boldsymbol{v}_\xi = \alpha \sum_{t=1}^{M} |\beta_t|^2$ for Scenario 2.

Additionally, define $\mathbf{f}(\boldsymbol{\theta}) = \left(\|\boldsymbol{p}\|^2 - 1, \Im(\boldsymbol{b}_a^\dagger \boldsymbol{p})\right)^T$, and consider the gradient vector of the constraints [21]

$$\boldsymbol{F}(\boldsymbol{\theta}) = \frac{\partial \mathbf{f}(\boldsymbol{\theta})}{\partial \boldsymbol{\theta}^T} = \begin{cases} \begin{bmatrix} 2\boldsymbol{\theta}_p^T & \mathbf{0}_{2M}^T \\ \\ \check{\boldsymbol{b}}_a^T & \mathbf{0}_{2M}^T \end{bmatrix} & \text{Scenario 1} \\ \\ \begin{bmatrix} 2\boldsymbol{\theta}_p^T & \mathbf{0}_2^T \\ \\ \check{\boldsymbol{b}}_a^T & \mathbf{0}_2^T \end{bmatrix} & \text{Scenario 2} \end{cases}$$

with $\check{\boldsymbol{b}}_a = [\Im(\boldsymbol{b}_a)^T, \Re(\boldsymbol{b}_a)^T]^T$. The above matrix has a full row rank if $\boldsymbol{\theta}_p$ and $\check{\boldsymbol{b}}_a$ are not proportional. Focusing on situations where such assumption is satisfied, there exists a matrix $\boldsymbol{U}_c$ such that

$$\boldsymbol{U}_c \boldsymbol{U}_c^T = \left(\boldsymbol{I}_{2(N+M)} - \boldsymbol{F}^T(\boldsymbol{\theta})\left(\boldsymbol{F}(\boldsymbol{\theta})\boldsymbol{F}^T(\boldsymbol{\theta})\right)^{-1}\boldsymbol{F}(\boldsymbol{\theta})\right), \qquad \boldsymbol{U}_c^T\boldsymbol{U}_c = \boldsymbol{I}_{2(N+M)-1} \qquad \text{Scenario 1}$$

$$\boldsymbol{U}_c \boldsymbol{U}_c^T = \left(\boldsymbol{I}_{2(N+1)} - \boldsymbol{F}^T(\boldsymbol{\theta})\left(\boldsymbol{F}(\boldsymbol{\theta})\boldsymbol{F}^T(\boldsymbol{\theta})\right)^{-1}\boldsymbol{F}(\boldsymbol{\theta})\right), \qquad \boldsymbol{U}_c^T\boldsymbol{U}_c = \boldsymbol{I}_{2(N+1)-1} \qquad \text{Scenario 2}$$

Hence, by Theorem 1 in [21], the error covariance $\boldsymbol{C}_{\boldsymbol{\theta}}$ of an unbiased estimate of $\boldsymbol{\theta}$ complies with

$$\boldsymbol{C}_{\boldsymbol{\theta}} \succeq \boldsymbol{U}_c(\boldsymbol{U}_c^T\boldsymbol{J}(\boldsymbol{\theta})\boldsymbol{U}_c)^{-1}\boldsymbol{U}_c^T\,,$$

for all $\boldsymbol{\theta}$ such that $\det(\boldsymbol{U}_c^T\boldsymbol{J}(\boldsymbol{\theta})\boldsymbol{U}_c) \neq 0$. As a by-product, the error covariance of an unbiased estimate of $\boldsymbol{\theta}_p$ fulfills

$$\boldsymbol{C}_{\boldsymbol{\theta}_p} \succeq [\boldsymbol{U}_c(\boldsymbol{U}_c^T\boldsymbol{J}(\boldsymbol{\theta})\boldsymbol{U}_c)^{-1}\boldsymbol{U}_c^T]_{\boldsymbol{\theta}_p,\boldsymbol{\theta}_p}\,, \tag{23}$$

with $[\boldsymbol{U}_c(\boldsymbol{U}_c^T\boldsymbol{J}(\boldsymbol{\theta})\boldsymbol{U}_c)^{-1}\boldsymbol{U}_c^T]_{\boldsymbol{\theta}_p,\boldsymbol{\theta}_p}$ the matrix formed by the first $2N$ rows and $2N$ columns of $\boldsymbol{U}_c(\boldsymbol{U}_c^T\boldsymbol{J}(\boldsymbol{\theta})\boldsymbol{U}_c)^{-1}\boldsymbol{U}_c^T$

Example. In this example, we study the Mean Square Error (MSE) of the proposed algorithm, i.e.

$$\text{MSE} = \frac{1}{N_{trials}}\sum_{t=1}^{N_{trials}} \|\boldsymbol{p}_{ML}^{(t)} - \boldsymbol{p}\|^2\,, \tag{24}$$

(where N_{trials} denotes the number of independent data realizations used to perform the MSE estimate and $\boldsymbol{p}_{ML}^{(t)}$ is the t-th ML estimate of $\boldsymbol{p}$) in comparison with the trace of the CRB matrix (right hand side of (23)). To this end, we assume $N = 5$, $M = 25$, covariance disturbance exponentially shaped with one-lag coefficient $\rho = 0.9$, elliptical constraint with $\boldsymbol{E} = \boldsymbol{I}/\epsilon$, $\boldsymbol{p} = \boldsymbol{p}_0 = \frac{1}{N}[1,\ldots,1]^T$. The convex optimization MATLAB toolbox SElf-DUal-MInimization (SeDuMi) [35] is exploited for solving the SDP problem involved in **Algorithm 1**.[8]

In Figure 2, MSE is plotted versus the Signal to Noise Ratio (SNR), i.e.

$$\text{SNR} = \sum_{t=1}^{M}|\alpha_t|^2\boldsymbol{p}_0^\dagger\boldsymbol{M}^{-1}\boldsymbol{p}_0\,, \tag{25}$$

for $N_{trials} = 1000$ and several values of the parameter ϵ. We observe that, as the SNR increases, the method's MSE approaches the trace of the constrained CRB matrix. Additionally, the lower the uncertainty (in this case the volume of the ellipsoid around the true steering direction), the better the performance.

IV. Applications

In this section, we present two applications of the estimation technique developed in the previous section. Precisely, we will focus on the problems of radar detection of range distributed targets with an elliptical steering constraint and robust point-target detection with a radar using a general antenna array configuration with a mix of high- and low-gain beams.

[8]The same solver is also exploited in the remaining simulations of the paper.

A. Detection of Range Distributed Targets with an Elliptical Steering Constraint

Assume that data are collected by an array of N sensors and deal with the problem of detecting the presence of a target across M range cells ($M \geq N$). Let $\boldsymbol{z}_t$, $t = 1, \ldots, M$, be the N-dimensional vector of the received signal from the t-th range cell (primary data). Assume that a secondary data set, $\boldsymbol{z}_t$, $t = M+1, \ldots, K$, is available and each of such snapshots does not contain any useful target echo.

The detection problem to be solved can be formulated in terms of the following binary hypotheses test:

$$\begin{cases} H_0 : \boldsymbol{z}_t = \boldsymbol{n}_t, \qquad t = 1, \ldots, K \\ \\ H_1 : \begin{cases} \boldsymbol{z}_t = \alpha_t \boldsymbol{p} + \boldsymbol{n}_t, & t = 1, \ldots, M \\ \boldsymbol{z}_t = \boldsymbol{n}_t, & t = M+1, \ldots, K \end{cases} \end{cases} \tag{26}$$

where

- α_t's are unknown parameters accounting for the useful target reflectivity and channel propagation effects;
- $\boldsymbol{n}_t$'s are N-dimensional disturbance vectors modeled as independent, zero-mean, complex Gaussian vectors with the same unknown covariance matrix, i.e.

$$E[\boldsymbol{n}_t \boldsymbol{n}_t^{\dagger}] = \boldsymbol{M}, \;\; t = 1, \ldots, K\,;$$

- $\boldsymbol{p}$ is the actual steering vector, which due to several effects might not be aligned with the nominal steering $\boldsymbol{s}$. In particular, in this application, we suppose that $\boldsymbol{p}$ belongs to the set $\Omega = \mathcal{U} \cap \mathcal{C}$ where $\mathcal{C} = \left\{ \boldsymbol{p} \in \mathbb{C}^N : (\boldsymbol{p} - \boldsymbol{p}_0)^{\dagger} \boldsymbol{E} (\boldsymbol{p} - \boldsymbol{p}_0) \leq 1 \right\}$, and $\boldsymbol{E}$ is a positive definite (or possibly semidefinite) matrix.

We investigate three possible statistical tests for the hypotheses test (26), i.e the one-step Generalized Likelihood Ratio Test (GLRT), the two-step GLRT, and the modified two-step GLRT, which in the absence of steering mismatches have been derived in [14].

One-Step GLRT. The one-step GLRT is the following decision rule

$$\frac{\max_{\boldsymbol{p} \in \Omega} \max_{\alpha_1, \ldots, \alpha_M} \max_{\boldsymbol{M}} f(\boldsymbol{z}_1, \ldots, \boldsymbol{z}_K | H_1, \alpha_1, \ldots, \alpha_M, \boldsymbol{p}, \boldsymbol{M})}{\max_{\boldsymbol{M}} f(\boldsymbol{z}_1, \ldots, \boldsymbol{z}_K | H_0, \boldsymbol{M})} \underset{H_0}{\overset{H_1}{\gtrless}} T, \tag{27}$$

where $f(\boldsymbol{z}_1, \ldots, \boldsymbol{z}_K | H_1, \alpha_1, \ldots, \alpha_M, \boldsymbol{p}, \boldsymbol{M})$ and $f(\boldsymbol{z}_1, \ldots, \boldsymbol{z}_K | H_0, \boldsymbol{M})$ are the data pdf's under H_1 and H_0 respectively, and T is the detection threshold set according to a design false alarm Probability (P_{fa}). Performing the maximizations over $\boldsymbol{M}$, $\alpha_1, \ldots, \alpha_M$, after some standard algebra, we obtain the following

decision rule

$$\max_{\boldsymbol{p}\in\Omega} \frac{\boldsymbol{p}^\dagger \boldsymbol{S}_s^{-1}\boldsymbol{Z}(\boldsymbol{I}+\boldsymbol{Z}^\dagger\boldsymbol{S}_s^{-1}\boldsymbol{Z})^{-1}\boldsymbol{Z}^\dagger\boldsymbol{S}_s^{-1}\boldsymbol{p}}{\boldsymbol{p}^\dagger\boldsymbol{S}_s^{-1}\boldsymbol{p}} \underset{H_0}{\overset{H_1}{\gtrless}} T\,, \tag{28}$$

where $\boldsymbol{Z}=[\boldsymbol{z}_1,\ldots,\boldsymbol{z}_M]$, $\boldsymbol{S}_s=\sum_{t=M+1}^{K}\boldsymbol{z}_t\boldsymbol{z}_t^\dagger$, and the same symbol T has been used to denote the modified threshold. Evidently, the optimization problem involved in the computation of the decision statistic can be solved resorting to the framework developed in the previous section based on the Charnes-Cooper transformation.

Two-Step GLRT. This two-step procedure first derives the GLRT based on primary data, assuming that the covariance matrix is known (step 1). Then, a fully adaptive detector is obtained by substituting the unknown matrix with the sample covariance matrix based on secondary data only (step 2). Step 1 can be accomplished evaluating

$$\frac{\max_{\boldsymbol{p}\in\Omega}\max_{\alpha_1,\ldots,\alpha_M} f(\boldsymbol{z}_1,\ldots,\boldsymbol{z}_M|H_1,\alpha_1,\ldots,\alpha_M,\boldsymbol{p},\boldsymbol{M})}{f(\boldsymbol{z}_1,\ldots,\boldsymbol{z}_M|H_0,\boldsymbol{M})} \underset{H_0}{\overset{H_1}{\gtrless}} T, \tag{29}$$

which, after some algebra leads to

$$\max_{\boldsymbol{p}\in\Omega} \frac{\boldsymbol{p}^\dagger \boldsymbol{M}^{-1}\boldsymbol{Z}\boldsymbol{Z}^\dagger\boldsymbol{M}^{-1}\boldsymbol{p}}{\boldsymbol{p}^\dagger\boldsymbol{M}^{-1}\boldsymbol{p}} \underset{H_0}{\overset{H_1}{\gtrless}} T\,. \tag{30}$$

Hence, a completely adaptive detector (step 2) can be obtained plugging $\boldsymbol{S}_s$ in place of $\boldsymbol{M}$, i.e.

$$\max_{\boldsymbol{p}\in\Omega} \frac{\boldsymbol{p}^\dagger \boldsymbol{S}_s^{-1}\boldsymbol{Z}\boldsymbol{Z}^\dagger\boldsymbol{S}_s^{-1}\boldsymbol{p}}{\boldsymbol{p}^\dagger\boldsymbol{S}_s^{-1}\boldsymbol{p}} \underset{H_0}{\overset{H_1}{\gtrless}} T\,. \tag{31}$$

The last maximization can be performed with the procedure of Section II.

Modified Two-Step GLRT. This modified two-step procedure first derives the GLRT based on primary data, assuming that the covariance structure $\boldsymbol{\Sigma}$ ($\boldsymbol{M}=\sigma^2\boldsymbol{\Sigma}$) is known (step 1). Then, a fully adaptive detector is obtained by substituting the sample covariance matrix in place of $\boldsymbol{\Sigma}$ (step 2).

Step 1 requires the computation of

$$\frac{\max_{\boldsymbol{p}\in\Omega}\max_{\alpha_1,\ldots,\alpha_M}\max_{\sigma^2} f(\boldsymbol{z}_1,\ldots,\boldsymbol{z}_M|H_1,\alpha_1,\ldots,\alpha_M,\boldsymbol{p},\sigma^2,\boldsymbol{\Sigma})}{\max_{\sigma^2} f(\boldsymbol{z}_1,\ldots,\boldsymbol{z}_M|H_0,\sigma^2,\boldsymbol{\Sigma})} \underset{H_0}{\overset{H_1}{\gtrless}} T, \tag{32}$$

which, after some algebra, can be recast as

$$\max_{\boldsymbol{p}\in\Omega} \frac{\boldsymbol{p}^\dagger \boldsymbol{\Sigma}^{-1}\boldsymbol{Z}\boldsymbol{Z}^\dagger\boldsymbol{\Sigma}^{-1}\boldsymbol{p}}{\mathrm{tr}\left(\boldsymbol{Z}^\dagger\boldsymbol{\Sigma}^{-1}\boldsymbol{Z}\right)\boldsymbol{p}^\dagger\boldsymbol{\Sigma}^{-1}\boldsymbol{p}} \underset{H_0}{\overset{H_1}{\gtrless}} T\,. \tag{33}$$

Plugging $\boldsymbol{S}_s$ in place of $\boldsymbol{\Sigma}$, we get the modified two-step GLRT, i.e.

$$\max_{\boldsymbol{p}\in\Omega} \frac{\boldsymbol{p}^\dagger \boldsymbol{S}_s^{-1}\boldsymbol{Z}\boldsymbol{Z}^\dagger \boldsymbol{S}_s^{-1}\boldsymbol{p}}{\mathrm{tr}\left(\boldsymbol{Z}^\dagger \boldsymbol{S}_s^{-1}\boldsymbol{Z}\right)\boldsymbol{p}^\dagger\boldsymbol{\Sigma}^{-1}\boldsymbol{p}} \underset{H_0}{\overset{H_1}{\gtrless}} T\,. \tag{34}$$

Again, **Algorithm 1** of Section II can be used to obtain the optimal value of the maximization problem in (34).

The new detectors (28), (31), and (34), will be respectively referred to as Elliptically Constrained One-Step GLRT (EC-1S-GLRT), EC Two-Step GLRT (EC-2S-GLRT), and EC Modified 2S-GLRT (EC-M2S-GLRT). Their counterparts, derived in [14] and assuming the perfect knowledge of $\boldsymbol{p}$, are instead respectively referred to as 1S-GLRT, 2S-GLRT, and M2S-GLRT.

In the following, we analyze the performance of the six considered receivers assuming $N = 5$, $K = 15$, $M = 3$, target uniformly spread within the M range cells, covariance disturbance exponentially shaped with one-lag coefficient $\rho = 0.9$, false alarm probability $P_{fa} = 10^{-2}$, $\boldsymbol{E} = \boldsymbol{I}/\epsilon$, and $\epsilon = 0.1$. As to the actual steering direction $\boldsymbol{p}$, we simulate it as follows

$$\boldsymbol{p} = \boldsymbol{p}_0 \cos\theta_m + \boldsymbol{p}_0^{\perp} \sin\theta_m\,,$$

where $\boldsymbol{p}_0^{\perp}$ denotes a (random) unit norm vector orthogonal to the nominal direction $\boldsymbol{p}_0$ and θ_m is a parameter which rules the degree of mismatch.

In Figure 3a, we plot the detection Probability P_d (evaluated through Montecarlo techniques) versus SNR (25) for $\theta_m = 0$, namely actual steering direction perfectly matched with the nominal one. The curves show that the receivers which know exactly the steering direction outperform the elliptically constrained detectors which assume some uncertainty on the actual steering direction. Indeed, for $P_d = 0.9$, the detection loss is always kept within 4 dB for all the three considered design strategies.

In Figure 3b, we consider the case where some mismatch is present. Precisely, we set $\theta_m = \mathrm{asin}\,(\sqrt{\epsilon}/2)$. Evidently, the classic receivers show a performance degradation which might also be severe for the cases of the 1S-GLRT and the M2S-GLRT. As to the elliptically constrained receivers, they exhibit a more robust behavior with respect to directional mismatches thanks to the uncertainty on the steering direction that they suppose at the design stage.

Finally, in Figure 3c, we analyze the effect of the parameter ϵ on the detection performance for $\theta_m = 0$. The plots show that the higher ϵ the higher the loss of each elliptically constrained receiver with respect to its counterpart which exactly knows the steering direction. This behavior can be explained observing that the higher ϵ the wider the uncertainty region where the actual steering vector is supposed to belong

to. Additionally, it seems that the EC-M2S-GLRT is the most sensitive among the new receivers, whereas the EC-1S-GLRT and EC-2S-GLRT exhibit almost the same degree of sensitivity.

B. Robust Point-Target Detection with a Radar using a General Antenna Array Configuration with a Mix of High- and Low-Gain Beams

Let us consider a radar operating with a general antenna array configuration [17] which includes a mix of high- and low-gain beams, obtained by suitable linear combinations of basic array elements. The radar is equipped with N independent receiving channels, each connected with one of the beams. According to the model developed in [17], the echoes collected by the N channels at the t-th sampling instant are stacked to form the N-dimensional vector $\boldsymbol{z}_t$, $t = 0, \ldots, K$ ($K + 1 \geq N$), referred to as t-th snapshot (for notational simplicity we assume that $\boldsymbol{z}_0$ contains the echo from the cell under test). As to the spatial behavior of the expected target, it is described by the N-dimensional steering vector $\boldsymbol{p}_\theta$ whose components are the complex amplitudes of the echo received at the N-th channel from a normalized target with direction of arrival θ. If the radar contains P high-gain beams then $\boldsymbol{p}_\theta = [\boldsymbol{p}^T, \boldsymbol{0}]^T$ ($\boldsymbol{p}$ is a P-dimensional column vector), since the usual signal received at the low-gain beams can be considered with a negligible power level [17].

The temporal behavior of the expected target echo is described by the $(K + 1)$-dimensional vector $\boldsymbol{s} = [s_0, s_1, \ldots, s_{K+1}]^T$ corresponding to the samples of the coded transmitted waveform (assumed, without loss of generality, with unit norm). Finally, the global disturbance is a combination of thermal noise and narrowband jammers. Hence, the $(K + 1)$ snapshots are modeled as independent complex Gaussian vectors with unknown covariance matrix $\boldsymbol{M}$ and mean $\alpha s_k \boldsymbol{p}_\theta$ under H_1 (0 under H_0) with α an unknown parameter accounting for the target backscattering and channel propagation effects.

Let us denote by

$$\boldsymbol{Z} = [\boldsymbol{z}_0, \ldots, \boldsymbol{z}_K]^T = \left[\begin{array}{c} \boldsymbol{Z}_h \\ \boldsymbol{Z}_l \end{array} \right],$$

where $\boldsymbol{Z}_h$ is a $P \times (K+1)$ matrix containing the P high-gain beams of each snapshot. The Generalized Likelihood Ratio (GLR) for known $\boldsymbol{p}$ can be written as [17]

$$\frac{\max_{\alpha, \boldsymbol{M}} f(\boldsymbol{Z}|H_1, \alpha, \boldsymbol{p}, \boldsymbol{M})}{\max_{\boldsymbol{M}} f(\boldsymbol{Z}|H_0, \boldsymbol{M})} = \left[1 - \frac{|\boldsymbol{p}^\dagger \boldsymbol{\Phi}^{-1} \boldsymbol{Y}_C \boldsymbol{s}^*|^2}{\left(1 + \boldsymbol{s}^T \boldsymbol{Z}^\dagger (\boldsymbol{Z} \boldsymbol{P}_s \boldsymbol{Z}^\dagger)^{-1} \boldsymbol{Z} \boldsymbol{s}^*\right) \boldsymbol{p}^\dagger \boldsymbol{\Phi}^{-1} \boldsymbol{p}} \right]^{-(K+1)} \tag{35}$$

where $\boldsymbol{P}_s = \boldsymbol{I} - \boldsymbol{s}^\star \boldsymbol{s}^T$, $\boldsymbol{\Phi} = \boldsymbol{Z}_h \boldsymbol{P}_s [\boldsymbol{I} - \boldsymbol{P}_s \boldsymbol{Z}_l^\dagger (\boldsymbol{Z}_l \boldsymbol{P}_s \boldsymbol{Z}_l^\dagger)^{-1} \boldsymbol{Z}_l \boldsymbol{P}_s] \boldsymbol{P}_s \boldsymbol{Z}_h^\dagger$, and $\boldsymbol{Y}_C = \boldsymbol{Z}_h [\boldsymbol{I} - \boldsymbol{P}_s \boldsymbol{Z}_l^\dagger (\boldsymbol{Z}_l \boldsymbol{P}_s \boldsymbol{Z}_l^\dagger)^{-1} \boldsymbol{Z}_l]$. Assuming that some uncertainty is available on $\boldsymbol{p}$, for instance due to array pointing errors or mis-calibration effects, one can resort to a further GLR over $\boldsymbol{p}$ in order to cope with the additional unknown

parameter. If an elliptical model, as that of the previous subsection, is considered for the uncertainty region, then the GLR becomes

$$\max_{\boldsymbol{p}\in\Omega}\left[1-\frac{|\boldsymbol{p}^\dagger\boldsymbol{\Phi}^{-1}\boldsymbol{Y}_C\boldsymbol{s}^*|^2}{\left(1+\boldsymbol{s}^T\boldsymbol{Z}^\dagger(\boldsymbol{Z}\boldsymbol{P}_s\boldsymbol{Z}^\dagger)^{-1}\boldsymbol{Z}\boldsymbol{s}^*\right)\boldsymbol{p}^\dagger\boldsymbol{\Phi}^{-1}\boldsymbol{p}}\right]^{-(K+1)} \tag{36}$$

which can be equivalently written as

$$\left[1-\frac{1}{\left(1+\boldsymbol{s}^T\boldsymbol{Z}^\dagger(\boldsymbol{Z}\boldsymbol{P}_s\boldsymbol{Z}^\dagger)^{-1}\boldsymbol{Z}\boldsymbol{s}^*\right)}\max_{\boldsymbol{p}\in\Omega}\frac{\boldsymbol{p}^\dagger\boldsymbol{\Phi}^{-1}\boldsymbol{Y}_C\boldsymbol{s}^*\boldsymbol{s}^T\boldsymbol{Y}_C^\dagger\boldsymbol{\Phi}^{-1}\boldsymbol{p}}{\boldsymbol{p}^\dagger\boldsymbol{\Phi}^{-1}\boldsymbol{p}}\right]^{-(K+1)}. \tag{37}$$

The maximization in (37) can be accomplished through **Algorithm 1** of Section II. From the above equation, we can construct the GLRT obtained comparing the GLR with a threshold, set in order to ensure the design P_{fa}. The resulting detector will be referred to as the EC-GLRT and is given by

$$\frac{1}{\left(1+\boldsymbol{s}^T\boldsymbol{Z}^\dagger(\boldsymbol{Z}\boldsymbol{P}_s\boldsymbol{Z}^\dagger)^{-1}\boldsymbol{Z}\boldsymbol{s}^*\right)}\max_{\boldsymbol{p}\in\Omega}\frac{\boldsymbol{p}^\dagger\boldsymbol{\Phi}^{-1}\boldsymbol{Y}_C\boldsymbol{s}^*\boldsymbol{s}^T\boldsymbol{Y}_C^\dagger\boldsymbol{\Phi}^{-1}\boldsymbol{p}}{\boldsymbol{p}^\dagger\boldsymbol{\Phi}^{-1}\boldsymbol{p}}\underset{H_0}{\overset{H_1}{\gtrless}}T. \tag{38}$$

Its counterpart, assuming the perfect knowledge of $\boldsymbol{p}$, will be instead referred to as the GLRT. In the following, we assess the performance of the EC-GLRT and the GLRT assuming that the actual steering direction is modeled as[9]

$$\alpha\boldsymbol{p}(i)=\alpha_1(1+a(i))\exp\left(j\pi\sin(\phi_p+\phi_m(i))\right)\qquad i=1,\ldots,P\,,$$

where $a(i)$ is a sequence of independent zero-mean Gaussian random variables with variance σ_a^2 and $\phi_m(i)$ is another sequence (statistically independent of $a(i)$) of independent zero-mean Gaussian random variables with variance σ_m^2. As to the disturbance scenario, we suppose the presence of noise plus two jammers impinging from 10 and 20 degrees respectively with a jammer to noise ratio of 20 dB.

In Figure 4a, we plot P_d (evaluated through Montecarlo techniques) of the two detectors versus SNR, i.e.

$$\text{SNR}=|\alpha|^2[\boldsymbol{p}_0^\dagger,\boldsymbol{0}^\dagger]\boldsymbol{M}^{-1}[\boldsymbol{p}_0^T,\boldsymbol{0}^T]^T\,,$$

where $\boldsymbol{p}_0$ is the nominal direction (i.e. $\boldsymbol{p}_0(i)=\frac{1}{\sqrt{P}}\exp\left(j\pi\sin(\phi_p)\right)$), $i=1,\ldots,P$, for $P_{fa}=10^{-2}$, $N=10$, $P=5$, $K=12$, $\epsilon=0.2$, $\phi_p=0$, $\sigma_a=0.1$, and two values of σ_m. The transmitted waveform $\boldsymbol{s}$ is a Barker code of length 13. For comparison purposes, the case of a perfect matched steering direction is plotted too.

The analysis of the curves shows that if a useful signal, perfectly matched to the nominal steering direction, impinges on the array, then the EC-GLRT exhibits almost the same P_d as the GLRT and,

[9]We are accounting for both amplitude and phase mismatch.

for $P_d > 0.9$, the respective performance curves overlap. When a mismatch is present, the EC-GLRT achieves a performance level better than the GLRT; specifically the stronger the mismatch the higher the detection gain.

The effect of the parameter σ_a is analyzed in Figure 4b, where P_d is plotted versus SNR for several values of σ_a, $\sigma_m = 3$, and the remaining simulation parameters as in Figure 4a. The plots highlight that the performance gain of the EC-GLRT over the GLRT depends on the entity of the amplitude mismatch; precisely, the higher the amplitude mismatch the higher the gain of the receiver which compensates for the amplitude mismatch. Summarizing, both the figures are a confirmation that, the elliptically constrained receiver is more robust than the counterpart with respect to directional mismatches.

V. Conclusions

In this paper, we have considered the problem of constrained steering direction estimation of a signal embedded in Gaussian disturbance. The constraint set has been represented in terms of a general quadratic inequality constraint which includes many situations of practical relevance such as conic constraints, elliptical constraints, exterior conic constraints, and exterior elliptical constraints. Additionally, a norm constraint accounting for the unitary norm of the steering direction has been considered. The estimation problem is attacked resorting to the ML criterion under two different assumptions for the received signal amplitude:

- the complex amplitude of the useful signal component changes from snapshot to snapshot;
- the useful signal keeps a constant amplitude within all the snapshots.

We have proved that the ML criterion leads in both cases to a fractional QCQP. In order to solve it, we have first relaxed the problem into a constrained fractional SDP problem which we prove equivalent to an SDP problem through the Charnes-Cooper transformation. Then, exploiting some rank-one decompositions, we have shown that the SDP relaxation is actually tight. Additionally, we have devised a procedure which constructs (in polynomial time) an optimal solution of the original problem from an optimal solution of the fractional SDP. We have also analyzed the quality of the derived estimator through a comparison of its performance with the constrained CRB. Finally, we have given two applications of the proposed theoretical framework in the context of radar detection of range distributed targets and robust point-target detection with a radar using a general antenna array configuration with a mix of high- and low-gain beams. In both the situations, the new procedure applies successfully.

Possible future research tracks might concern the application of the framework to additional statistical signal processing problems involving Over The Horizon (OTH) radar or Synthetic Aperture Radar (SAR)

processing (including atmospheric effects) as well as the extension of the procedure to account for the presence of a specific structure in the steering direction.

APPENDIX

A. Proof of Lemma 3.1

Proof: Observe that the feasible region of $\mathcal{P}_3$

$$\Omega' = \{\boldsymbol{W} \succeq \boldsymbol{0} \mid \mathrm{tr}(\boldsymbol{Q}_1\boldsymbol{W}) \geq 0,\, \mathrm{tr}(\boldsymbol{Q}_2\boldsymbol{W}) = 1,\, \mathrm{tr}(\boldsymbol{Q}_3\boldsymbol{W}) = 1\} \tag{39}$$

is a closed subset of the compact set

$$\Omega'' = \{\boldsymbol{W} \succeq \boldsymbol{0} \mid \mathrm{tr}\left((\boldsymbol{Q}_2 + \boldsymbol{Q}_3)\boldsymbol{W}\right) = \mathrm{tr}(\boldsymbol{W}) = 2\},$$

thus the set Ω' is compact as well. Also note that the denominator and numerator of the objective function of the fractional SDP $\mathcal{P}_3$ are continuous, and that the denominator is positive over the feasible region (because $\mathrm{tr}(\boldsymbol{Q}_0\boldsymbol{W}) > 0$ for any $\boldsymbol{W}$ belonging to the set $\{\boldsymbol{W} \succeq \boldsymbol{0} \mid \mathrm{tr}(\boldsymbol{Q}_2\boldsymbol{W}) = 1\}$ which includes the feasible region). Let $\Omega''' = \{\boldsymbol{W} \succeq 0 |\ \mathrm{tr}(\boldsymbol{Q}_2\boldsymbol{W}) = 1\}$. Then, for any $\boldsymbol{W} \in \Omega'$, we have that

$$0 \leq \mathrm{tr}\left(\boldsymbol{Q}_{-1}\boldsymbol{W}\right) \leq \underset{\boldsymbol{W} \in \Omega'''}{\mathsf{maximize}}\ \mathrm{tr}\left(\boldsymbol{Q}_{-1}\boldsymbol{W}\right) = \lambda_{\max}(\boldsymbol{M}^{-1}\boldsymbol{S}\boldsymbol{M}^{-1})$$

and

$$\lambda_{\min}(\boldsymbol{M}^{-1}) = \underset{\boldsymbol{W} \in \Omega'''}{\mathsf{minimize}}\ \mathrm{tr}\left(\boldsymbol{Q}_0\boldsymbol{W}\right) \leq \mathrm{tr}\left(\boldsymbol{Q}_0\boldsymbol{W}\right) \leq \underset{\boldsymbol{W} \in \Omega'''}{\mathsf{maximize}}\ \mathrm{tr}\left(\boldsymbol{Q}_0\boldsymbol{W}\right) = \lambda_{\max}(\boldsymbol{M}^{-1})\ .$$

This implies that the objective function of problem $\mathcal{P}_3$ is finite-valued over the feasible region. It follows from Weierstrass' Theorem (for instance, see [36, Chapter 2]) that problem $\mathcal{P}_3$ has always an optimal solution. Hence the problem is solvable. ■

B. Proof of Lemma 3.2

Proof: The dual of SDP $\mathcal{P}_4$ is

$$\mathcal{P}_d \begin{cases} \underset{y_0,y_1,y_2,y_3}{\mathsf{minimize}} & y_0 \\ \mathsf{subject\ to} & \boldsymbol{Q}_{-1} - y_0\boldsymbol{Q}_0 - y_1\boldsymbol{Q}_1 - y_2\boldsymbol{Q}_2 - y_3\boldsymbol{Q}_3 \preceq \boldsymbol{0} \\ & y_2 + y_3 \leq 0 \\ & y_1 \leq 0. \end{cases} \tag{40}$$

Since $\mathcal{P}_3$ has an optimal solution, say $\boldsymbol{X}^\star$, hence it is easily seen that $(\boldsymbol{X}^\star/\text{tr}(\boldsymbol{Q}_0\boldsymbol{X}^\star), 1/\text{tr}(\boldsymbol{Q}_0\boldsymbol{X}^\star))$ is feasible for $\mathcal{P}_4$. Therefore, by weak duality, Problem $\mathcal{P}_d$ is bounded below. Assume that $y_1 = \epsilon_1 < 0$ and $y_2 = \epsilon_2 < 0$ are given such that $\epsilon_2 - \epsilon_1 c < 0$. Then

$$\boldsymbol{Q}_{-1} - y_0\boldsymbol{Q}_0 - y_1\boldsymbol{Q}_1 - y_2\boldsymbol{Q}_2 - y_3\boldsymbol{Q}_3 = \left[\begin{array}{cc} \boldsymbol{M}^{-1}\boldsymbol{S}\boldsymbol{M}^{-1} - y_0\boldsymbol{M}^{-1} - \epsilon_1\boldsymbol{A} - \epsilon_2\boldsymbol{I} & -\epsilon_1\boldsymbol{b} \\ -\epsilon_1\boldsymbol{b}^\dagger & -\epsilon_1 c - y_3 \end{array}\right] \preceq \boldsymbol{0},$$

which is equivalent to

$$\left[\begin{array}{cc} y_0\boldsymbol{M}^{-1} + \epsilon_1\boldsymbol{A} + \epsilon_2\boldsymbol{I} - \boldsymbol{M}^{-1}\boldsymbol{S}\boldsymbol{M}^{-1} & \epsilon_1\boldsymbol{b} \\ \epsilon_1\boldsymbol{b}^\dagger & \epsilon_1 c + y_3 \end{array}\right] \succeq \boldsymbol{0}.$$

Now, we can set $y_0 > 0$ to be sufficiently large and set y_3 so that $\epsilon_1^2\boldsymbol{b}^\dagger(y_0\boldsymbol{M}^{-1} + \epsilon_1\boldsymbol{A} + \epsilon_2\boldsymbol{I} - \boldsymbol{M}^{-1}\boldsymbol{S}\boldsymbol{M}^{-1})^{-1}\boldsymbol{b}$ is close enough to zero, and $y_3 > \epsilon_1^2\boldsymbol{b}^\dagger(y_0\boldsymbol{M}^{-1} + \epsilon_1\boldsymbol{A} + \epsilon_2\boldsymbol{I} - \boldsymbol{M}^{-1}\boldsymbol{S}\boldsymbol{M}^{-1})^{-1}\boldsymbol{b} - \epsilon_1 c$ and $y_3 + y_2 = y_3 + \epsilon_2 < 0$. This means the SDP problem $\mathcal{P}_d$ is strictly feasible. It follows from the strong duality theorem (for example, see [32, Theorem 1.7.1]) that Problem $\mathcal{P}_4$ is solvable. ■

C. Proof of Lemma 3.3

Proof: Suppose that $\boldsymbol{W}^\star$ is an optimal solution of $\mathcal{P}_3$ and $v(\mathcal{P}_3)$ is the optimal value of $\mathcal{P}_3$, and that $v(\mathcal{P}_4)$ is the optimal value of $\mathcal{P}_4$. It is verified easily that $(\boldsymbol{W}^\star/\text{tr}(\boldsymbol{Q}_0\boldsymbol{W}^\star), s^\star)$ with $s^\star = 1/\text{tr}(\boldsymbol{Q}_0\boldsymbol{W}^\star)$ is feasible for $\mathcal{P}_4$, and the objective function value at the feasible point is $\text{tr}(\boldsymbol{Q}_{-1}\boldsymbol{W}^\star)/\text{tr}(\boldsymbol{Q}_0\boldsymbol{W}^\star) = v(\mathcal{P}_3)$. Thus, we have $v(\mathcal{P}_4) \geq v(\mathcal{P}_3)$.

On the other hand, let $(\boldsymbol{X}^\star, s^\star)$ be an optimal solution of $\mathcal{P}_4$. We claim that $s^\star > 0$. Indeed, if $s^\star = 0$, then $\text{tr}(\boldsymbol{Q}_2\boldsymbol{X}^\star) + \text{tr}(\boldsymbol{Q}_3\boldsymbol{X}^\star) = \text{tr}(\boldsymbol{X}^\star) = 2s^\star = 0$, which implies $\boldsymbol{X}^\star = \boldsymbol{0}$. This is impossible since $\text{tr}(\boldsymbol{Q}_0\boldsymbol{X}^\star) = 1$. It is checked that $\boldsymbol{X}^\star/s^\star$ is feasible for $\mathcal{P}_3$, and the objective function value of $\mathcal{P}_3$ at the feasible point is $\text{tr}\left(\boldsymbol{Q}_{-1}(\boldsymbol{X}^\star/s^\star)\right)/\text{tr}\left(\boldsymbol{Q}_0(\boldsymbol{X}^\star/s^\star)\right) = \text{tr}(\boldsymbol{Q}_{-1}\boldsymbol{X}^\star)/\text{tr}(\boldsymbol{Q}_0\boldsymbol{X}^\star) = \text{tr}(\boldsymbol{Q}_{-1}\boldsymbol{X}^\star) = v(\mathcal{P}_4)$. Therefore, we have $v(\mathcal{P}_3) \geq v(\mathcal{P}_4)$, which yields $v(\mathcal{P}_3) = v(\mathcal{P}_4)$. ■

REFERENCES

[1] S. A. Vorobyov, A. B. Gershman, and Z. Luo, "Robust Adaptive Beamforming Using Worst-Case Performance Optimization: A Solution to the Signal Mismatch Problem," *IEEE Trans. on Signal Processing*, Vol. 51, No. 2, pp. 313-324, February 2003.

[2] P. Stoica, Z. Wang, and J. Li, "Robust Capon Beamforming," *IEEE Signal Processing Letters*, Vol. 10, No. 6, pp. 172-175, June 2003.

[3] J. Li, P. Stoica, and Z. Wang, "On Robust Capon Beamforming and Diagonal Loading," *IEEE Trans. on Signal Processing*, Vol. 51, No. 7, pp. 1702-1715, July 2003.

[4] J. Li, P. Stoica, and Z. Wang, "Doubly Constrained Robust Capon Beamformer," *IEEE Trans. on Signal Processing*, Vol. 52, No. 9, pp. 2407-2423, September 2004.

[5] A. Beck and Y. C. Eldar, "Doubly Constrained Robust Capon Beamformer with Ellipsoidal Uncertainty Sets," *IEEE Trans. on Signal Processing*, Vol. 55, No. 2, pp. 753-758, January 2007.

[6] S. Ramprashad, T. W. Parks, and R. Shenoy, "Signal Modeling and Detection Using Cone Classes," *IEEE Trans. on Signal Processing*, Vol. 44, No. 2, pp. 329-338, February 1996.

[7] M. N. Desai and R. S. Mangoubi, "Adaptive Robust Constrained Matched Filter and Subspace Detection," *Proc. of 36th Asilomar Conference on Signals, Systems, and Computers*, Pacific Grove, CA, November 2002, pp. 768-772.

[8] M. N. Desai and R. S. Mangoubi, "Robust Gaussian and non-Gaussian matched subspace detection," *IEEE Trans. on Signal Processing*, Vol. 51, No. 12, pp. 3115-3127, December 2003.

[9] F. Bandiera, A. De Maio, and G. Ricci, "Adaptive CFAR Radar Detection with Conic Rejection," *IEEE Trans. on Signal Processing*, Vol. 55, No. 6, pp. 2533 - 2541, June 2007.

[10] O. Besson, "Detection of a Signal in Linear Subspace with Bounded Mismatch," *IEEE Trans. on Aerospace and Electronic Systems*, Vol. 42, No. 3, pp. 1131 - 1139, July 2006.

[11] O. Besson: "Adaptive Detection With Bounded Steering Vectors Mismatch Angle," *IEEE Trans. on Signal Processing*, Vol. 55, No. 4, pp. 1560-1564, April 2007.

[12] A. De Maio, S. De Nicola, Y. Huang, S. Zhang, and A. Farina, "Adaptive Detection and Estimation in the Presence of Useful Signal and Interference Mismatches," *IEEE Trans. on Signal Processing*, Vol. 57, No. 2, pp. 436-450, February 2009.

[13] K. Gerlach and M. J. Steiner, "Adaptive Detection of Range Distributed Targets," *IEEE Trans. on Signal Processing*, Vol. 47, No. 7, pp. 1844-1851, July 1999.

[14] E. Conte, A. De Maio, and G. Ricci, "GLRT-based Adaptive Detection Algorithms for Range Spread Targets," *IEEE Trans. on Signal Processing*, Vol. 49, No. 7, pp. 1336 - 1348, July 2007.

[15] L. Xu, J. Li, and P. Stoica, "Target Detection and Parameter Estimation for MIMO Radar Systems," *IEEE Trans. on Aerospace and Electronic Systems* , Vol. 44, No. 3, pp. 927 - 939, July 2008.

[16] J. Li and P. Stoica, *MIMO Radar Signal Processing*, John Wiley & Sons, Inc., Publication, 2008.

[17] A. Farina, P. Lombardo, and L. Ortenzi, "A Unified Approach to Adaptive Radar Processing with General Antenna Array Configuration," *Signal Processing*, Vol. 84, No. 9, pp. 1593 - 1623, September 2004.

[18] A. Charnes and W. W. Cooper, "Programming with Linear Fractional Functionals," *Naval Research Logistics Quarterly*, Vol. 9, pp. 181-186, 1962.

[19] W. Ai, Y. Huang, and S. Zhang, "Further Results on Rank-One Matrix Decomposition and Its Applications," accepted for publication by *Mathematical Programming*, January 2008.

[20] Y. Huang and S. Zhang, "Complex Matrix Decomposition and Quadratic Programming," *Mathematics of Operations Research*, Vol. 32, No. 3, pp. 758-768, Aug. 2007.

[21] P. Stoica and B. C. Ng, "On the Cramér-Rao Bound under Parametric Constraints," *IEEE Signal Processing Letters*, Vol. 5, No. 7, pp. 177 - 179, 1998.

[22] W.-K. Ma, T. N. Davidson, K. M. Wong, Z.-Q. Luo, and P. C. Ching, "Quasi-Maximum-Likelihood Multiuser Detection using Semi-Definite Relaxation with Applications to Synchronous CDMA," *IEEE Trans. on Signal Processing*, Vol. 50, No. 4, pp. 912-922, April 2002.

[23] Y. Yang, C. Zhao, P. Zhou, and W. Xu, "MIMO Detection of 16-QAM Signaling based on Semidefinite Relaxation," *IEEE Signal Processing Letters*, Vol. 14, No. 11, pp. 797-800, November 2007.

[24] N. D. Sidiropoulos and Z.-Q. Luo, "A Semidefinite Relaxation Approach to MIMO Detection for High-Order QAM Constellations," *IEEE Signal Processing Letters*, Vol. 13, No. 9, pp. 525-528, September 2006.

[25] J. Li, J. R. Guerci, and L. Xu, "Signal Waveform's Optimal-under-Restriction Design for Active Sensing", *IEEE Signal Processing Letters*, Vol. 13, No. 9, pp. 565-568, September 2006.

[26] R. G. Lorentz and S. Boyd, "Robust Minimum Variance Beamforming," *IEEE Trans. on Signal Processing*, Vol. 53, No. 5, pp. 1684-1696, May 2005.

[27] N. B. Pulsone and C. M. Rader, "Adaptive Beamformer Orthogonal Rejection Test," *IEEE Trans. on Signal Processing*, Vol. 49, No. 3, pp. 521-529, March 2001.

[28] F. Bandiera, D. Orlando, and G. Ricci, "Advanced Radar Detection Schemes under Mismatched Signal Models," *Synthesis Lectures on Signal Processing N. 8, Morgan & Claypool Publishers*, March 2009.

[29] J. P. Crouzeix, and J. A. Ferland, "Algorithms for Generalized Fractional Programming, " *Mathematical Programming*, Vol. 52, pp. 191 - 207, 1991.

[30] A. I. Barros, J. B .G. Frenk, S. Schaible, and S. Zhang, "A New Algorithm for Generalized Fractional Programs," *Mathematical Programming*, Vol. 72, pp. 147 - 175, 1996.

[31] S. Boyd and L. Vandenberghe, "*Convex Optimization*," Cambridge University Press, New York, First published 2004, Sixth printing with corrections 2008.

[32] A. Nemirovski, "*Lectures on Modern Convex Optimization*," Class Notes, Georgia Institute of Technology, Fall 2005.

[33] J. D. Gorman and A. O. Hero, "Lower Bounds for Parametric Estimation with Constraints," *IEEE Trans. on Information Theory*, Vol. 26, pp. 1285 - 2301, Nov 1990.

[34] S. M. Kay, *Fundamentals of Statistical Signal Processing: Estimation Theory*, Upper Saddle River, NJ: Prentice Hall, 1993, Vol 1.

[35] J. F. Sturm, " Using SeDuMi 1.02, a MATLAB Toolbox for Optimization over Symmetric Cones," *Optimization Methods and Software*, Vol. 11-12, pp. 625-653, Aug. 1999.

[36] D. P. Bertsekas, A. Nedic and A. E. Ozdaglar, "*Convex Analysis and Optimization*," Athena Scientific, 2003

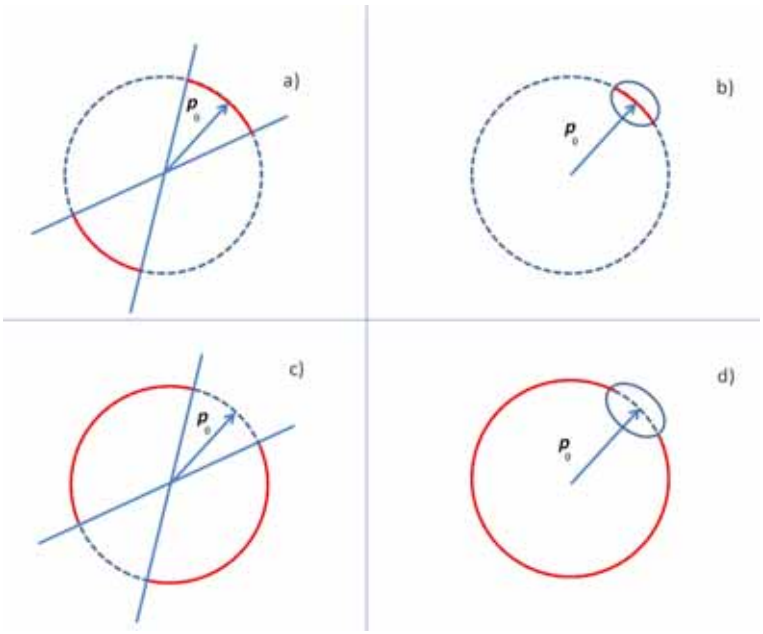

Figure 1: Pictorial description of the set Ω for $N = 2$ and real observations.

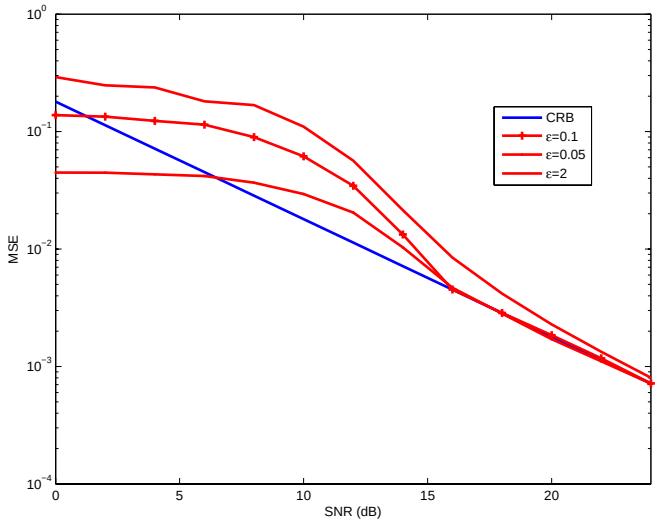

Figure 2: MSE versus SNR for $N = 5$, $M = 25$, perfectly matched steering direction, and several values of ϵ. Trace of the constrained CRB matrix (right hand side of (23)) solid line. $\epsilon = 0.05$ o-marked curve. $\epsilon = 0.1$ +-marked curve. $\epsilon = 2$ star-marked curve.

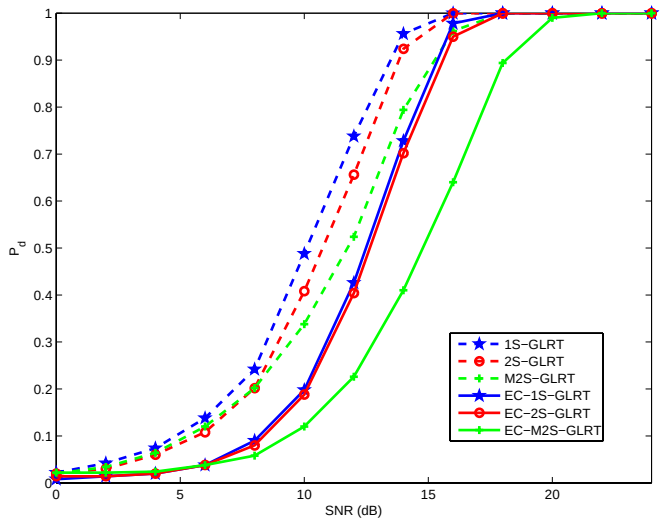

Figure 3a: P_d versus SNR for $P_{fa} = 10^{-2}$, $N = 5$, $K = 15$, $M = 3$, $\epsilon = 0.1$, and perfectly matched steering direction. 1S-GLRT (dashed star-marked curve), 2S-GLRT (dashed o-marked curve), M2S-GLRT (dashed +-marked curve), EC-1S-GLRT (solid star-marked curve), EC-2S-GLRT (solid o-marked curve), EC-M2S-GLRT (solid +-marked curve).

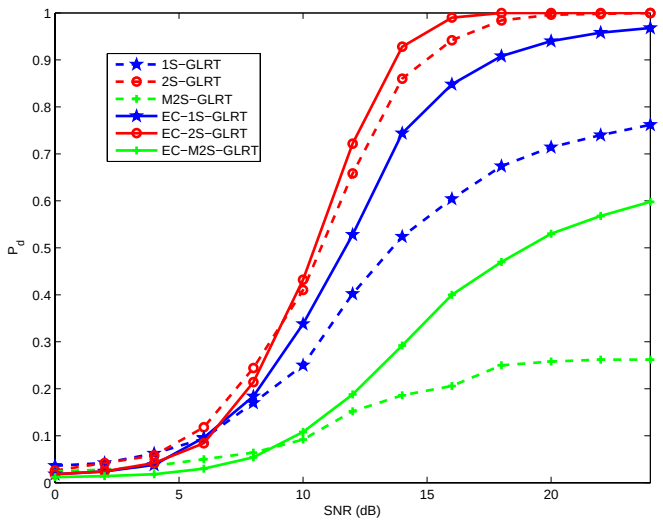

Figure 3b: P_d versus SNR for $P_{fa} = 10^{-2}$, $N = 5$, $K = 15$, $M = 3$, $\epsilon = 0.1$, mismatched steering direction with $\theta_m = \text{asin}\,(\sqrt{\epsilon}/2)$. 1S-GLRT (dashed star-marked curve), 2S-GLRT (dashed o-marked curve), M2S-GLRT (dashed +-marked curve), EC-1S-GLRT (solid star-marked curve), EC-2S-GLRT (solid o-marked curve), EC-M2S-GLRT (solid +-marked curve).

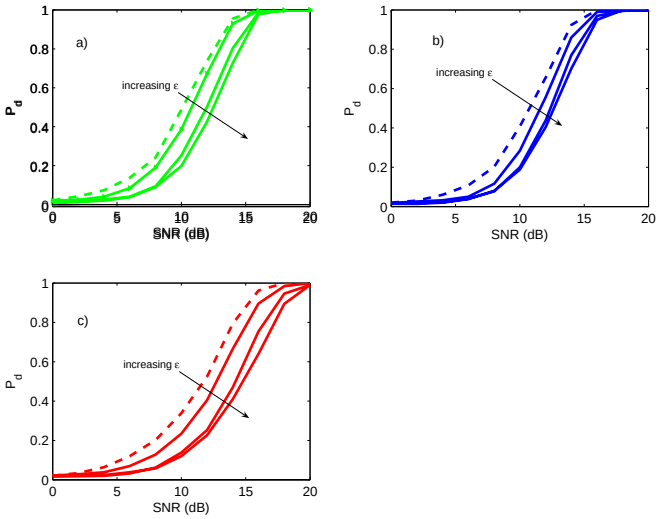

Figure 3c: P_d versus SNR for $P_{fa} = 10^{-2}$, $N = 5$, $K = 15$, $M = 3$, perfectly matched steering direction, and several values of $\epsilon \in \{0.1, 0.05, 0.01\}$. Subplot a) 1S-GLRT (dashed curve) and EC-1S-GLRT (solid curves). Subplot b) 2S-GLRT (dashed curve) and EC-2S-GLRT (solid curves). Subplot c) M2S-GLRT (dashed curve) and EC-M2S-GLRT (solid curves).

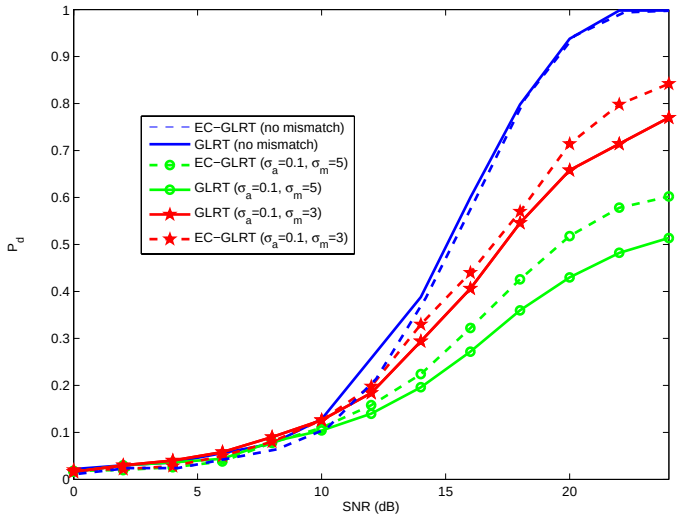

Figure 4a: P_d versus SNR for $P_{fa} = 10^{-2}$, $N = 10$, $P = 5$, $K = 12$, $\epsilon = 0.2$, mismatched steering direction with $\sigma_a = 0.1$ and two values of σ_m ($\sigma_m = 3$ star-marked curves and $\sigma_m = 5$ o-marked curves). GLRT (solid curves), EC-GLRT (dashed curves).

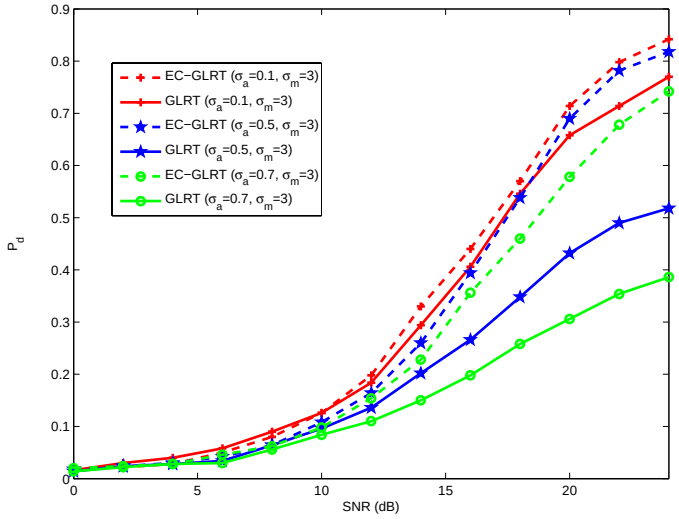

Figure 4b: P_d versus SNR for $P_{fa} = 10^{-2}$, $N = 10$, $P = 5$, $K = 12$, $\epsilon = 0.2$, mismatched steering direction with $\sigma_m = 3$ and three values of σ_a ($\sigma_a = 0.1$ +-marked curves, $\sigma_a = 0.5$ star-marked curves, and $\sigma_a = 0.7$ o-marked curves.